



# Hydrodynamic optimisation of a new hull bow shape by CFD code

**Media Rafik**

**Master Thesis**

presented in partial fulfillment  
of the requirements for the double degree:  
“Advanced Master in Naval Architecture” conferred by University of  
Liege

“Master of Sciences in Applied Mechanics, specialization in  
Hydrodynamics, Energetics and Propulsion” conferred by Ecole  
Centrale de Nantes  
developed at University of Genoa,  
in the framework of the

**“EMSHIP”  
Erasmus Mundus Master Course  
in “Integrated Advanced Ship Design”**

Supervisor : Prof. Dario Boote, University of Genoa

Reviewer : Prof. Lionel Gentaz, University of Ecole Central de Nantes

February 2015





## **Abstract**

### Hydrodynamic optimisation of a new hull bow shape by CFD code

By Media Rafik

As ship resistance is a major concern for ship design in terms of energy consumption and hydrodynamic aspects of ship, there is a project to look for the best ship designs and also for the optimisation methods which can be the most effective. Starting from the last two decades, optimisation methods are growing in a significant rate as well as the CAD driven simulation software.

The aim of this work is to check the usefulness of adapting a new bulbous bow for a hull of a military frigate, for three operational speeds with a maximum speed of 25 knots. The bulbous bow is known to reduce the drag resistance due to its influence on the bow wave system. For this optimisation process RANS-CFD code of STAR-CCM+ is used to calculate the drag forces on the hull of ship. An open source CAD software based on the parametric design method has been used to generate the bulbous bow shapes for the purpose of testing and evaluation of objectives.

The obtained CFD results are compared to towing tank test results for a hull without bulbous bow.

**Keywords:** Drag resistance, bulbous bow, optimisation, STAR-CCM+, CAD software



## **ACKNOWLEDGEMENTS**

Firstly, I am very thankful to Erasmus Mundus EMSHIP program who has given me this chance to participate in this master; it was a nice opportunity to upgrade in ship design field.

The author would like to thank the supervisor Professor Dario Boote and the support of its academic staff during the semester in the Polo University of La Spezia.

Also big thank for the direction of Computational Fluid Dynamic Laboratory which provides the all the needed support to do this work.

Particular thanks go also to Intermarine engineering staff and his head Mr. Mariotti for the good collaboration and the help during this project.

Finally, I don't forget to thank all professors from ULg of liege, ECN of Nantes and UNIGE particularly POLO university in La Spezia.

This master thesis was developed in the frame of the European Master Course in "Integrated Advanced Ship Design" named "EMSHIP" for "European Education in Advanced Ship Design", Ref. 159652-1-2009-1-BE-ERA MUNDUS-EMMC

## Contents

1	Chapter 1 .....	1-12
	Introduction .....	1-12
	1.1 Introduction .....	1-12
	1.2 History about Bulbous .....	1-12
	1.3 State of Art.....	1-15
2	Chapter 2.....	2-16
	Theoretical Background .....	2-16
	2.1 Bulb forms .....	2-16
	2.1.1 Bulbous bow projecting above CWL .....	2-17
	2.1.2 Projecting length: .....	2-18
	2.1.3 Bulb axis.....	2-18
	2.1.4 Area ratio .....	2-18
	2.1.5 Transition .....	2-19
	2.2 Power requirements with bulbous bow .....	2-19
	2.3 Parametric ship design.....	2-21
	2.3.1 Parameters of design: .....	2-22
3	Chapter 3.....	3-24
	Principles of CFD.....	3-24
	3.1 Resistance Calculation with RANS CFD Methods .....	3-24
	3.2 Governing equations.....	3-24
	3.3 Turbulent boundary layer .....	3-26
	3.4 Courant number .....	3-27
4	Chapter 4.....	4-28
	4.1 Resistance of bear hull.....	4-28
	4.2 Overset mesh .....	4-29
	4.3 Results for Resistance for three speeds .....	4-32
	4.4 Comparison of resistance results .....	4-37
5	Chapter 5.....	5-39

## Hydrodynamic optimisation of new hull bow shape by CFD code

Optimisation tests.....	5-39
5.1 Work flow.....	5-39
5.2 Base design.....	5-40
5.3 Calculating total resistance of base design.....	5-41
5.4 Generating designs for simulation test.....	5-44
5.4.1 Vehicle Sketch Pad (VSP).....	5-44
5.5 Design of experiments.....	5-45
5.6 Results of first design tests.....	5-48
6 Discussions and Conclusion.....	6-51
6.1 Discussion of results:.....	6-51
6.2 Conclusion:.....	6-52
References:.....	6-53

## List of Figures:

Figure 1: Diagram that relates the evolution of the application of bulbs as a function of the Froude Number, along the XX century .....	1-14
Figure 2 : Modern bulb shapes .....	2-16
Figure 3 : Bulb types .....	2-16
Figure 4: Position of forward perpendicular with high bulbous bows .....	2-17
Figure 5: Length of freeboard calculation with low freeboard deck .....	2-17
Figure 6: Bulb with projecting length. Theoretical bulb section area of the forward perpendicular .....	2-19
Figure 7: Fin bulb .....	2-20
Figure 8: Resistance comparison (ship with and without bulbous bow).....	2-21
Figure 9: Dimensionless bulbous bow parameters as defined by Kracht .....	2-22
Figure 10 : Parameters of optimisation of bulbous .....	2-23
Figure 11: Hull form without bulbous of studied case .....	4-29
Figure 12: Volume mesh of bare hull on STAR-CCM+ .....	4-30
Figure 13: Overset cell status of the background region.....	4-31
Figure 14: Wall Y+ contour field for wall function .....	4-31
Figure 15: Courant number used in simulations .....	4-32
Figure 16: Drag and lift developpement with respect to time for 25 knots.....	4-33
Figure 17: Drag and lift developpement with respect to time for 20 knots.....	4-33
Figure 18: Drag and lift developpement with respect to time for 15 knots.....	4-34



## Hydrodynamic optimisation of new hull bow shape by CFD code

Figure 19: Wave pattern for bare hull for 25 knots .....	4-34
Figure 20: Wave pattern for bare hull for 20 knots .....	4-35
Figure 21: Wave pattern for bare hull for 15 knots .....	4-35
Figure 22: Trim angle for bare hull for 25knots.....	4-36
Figure 23: Heave motion for bare hull for 25 knots.....	4-36
Figure 24: Comparison between results of STAR-CCM+ and Holtrop 84 for bare hull .....	4-37
Figure 25: STAR-CCM+ vs different power prediction methods for hull with appendages & hull roughness .....	4-38
Figure 26: Base design of bulbous bow .....	5-40
Figure 27: Ship base design .....	5-40
Figure 28: Mesh of base bulbous design .....	5-41
Figure 29: Wave pattern around the ship for base design .....	5-41
Figure 30: Wave pattern around the bare hull .....	5-42
Figure 31: Drag and lift forces acting on base design for 25knts.....	5-43
Figure 32: Drag and lift forces acting on Bare hull for 25knts .....	5-43
Figure 33: VSP overview task.....	5-44
Figure 34: Parameters define generating design samples .....	5-45
Figure 35 : DOE design of experiments represented by Lb versus Bb .....	5-48
Figure 36 : DOE design of experiments represented by Lb versus Hb.....	5-48
Figure 37 : Drag Resistance for different Lb of design individuals.....	5-49
Figure 38: Drag Resistance for different Hb height of design individuals .....	5-49
Figure 39: Drag Resistance for different Bb breadth of design individuals.....	5-50

Figure 40 : Comparison of improvement in drag reduction with reference to bare hull.....5-50

## List of Tables:

Table 1 Main Dimensions and data of the ship .....4-28

Table 2 Design individuals' shapes and parameters .....5-46

Table 3 Design individuals' shapes and parameters .....5-47

***Declaration of Authorship***

I declare that this thesis and the work presented in it are my own and have been generated by me as the result of my own original research.

Where I have consulted the published work of others, this is always clearly attributed.

Where I have quoted from the work of others, the source is always given. With the exception of such quotations, this thesis is entirely my own work.

I have acknowledged all main sources of help.

Where the thesis is based on work done by myself jointly with others, I have made clear exactly what was done by others and what I have contributed myself.

This thesis contains no material that has been submitted previously, in whole or in part, for the award of any other academic degree or diploma.

I cede copyright of the thesis in favor of the Intermarine Spa Company

Geneva in January 20<sup>th</sup>, 2015

Signature: *Media Rafik*

# Chapter 1

## Introduction

---

### 1.1 Introduction

The optimisation of the bow part of ship is becoming a very useful tool for reduction of the drag resistance for ships, whether it is for a design stage or in retrofitting project of an existent ship, this is especially successful with the help of the development of the numerical methods applied in this field of optimisation, the CAD software's able to create designs with more applicable purposes and CFD solver codes approaching the numerical solutions to be closer to fluid reality.

In general, the adaptation of a new bow shape for a ship will help to improve the ship to be more efficient by providing better hydrodynamic performances. CFD simulations nowadays are reliable and highly used to determine the resistance and the flow characteristics around the ship, This can be very helpful for understanding some effects on the special parts of ship as example of screws or bow thrusters, in comparison with tests in towing tanks which are more costly and usually used for determination of characteristics of the last product.

The present work will be dedicated to adapting of a bulbous bow for a military frigate of 75m.

This project needs to look the best bow shape with keeping the main characteristics of speed and hull shape conserved as the preliminary design. Since it has appendages as bow thrusters and twin screw, this needs more caring in order not to generate a flow disturbing the work of these appendages.

### 1.2 History about Bulbous

The bulbous bow originated in the bow ram named (esporao), a structure of military nature utilized in war ships on the end of the 19th century and beginning of the 20th century.

The bulbous bow was allegedly invented in the David Taylor Model Basin (DTMB) in the EUA.

The first bulbous bows appeared in the 1920s with the "Bremen" and the "Europa", two German passenger ships built to operate in the North Atlantic. The "Bremen", built in 1929, won the Blue Riband of the crossing of the Atlantic with the speed of 27.9 knots.

## Hydrodynamic optimisation of new hull bow shape by CFD code

Other smaller passenger ships, such as the American “President Hoover” and “President Coolidge” of 1931, started to appear with bulbous bows although they were still considered as experimental, by ship owners and shipyards. • In 1935, the “Normandie”, built with a bulbous bow, attained the 30 knots.

In Japan some navy ships from WWII such as the cruiser “Yamato” (1940) used already bulbous bows. The systematic research started on the late 1950s. The “Yamashiro Maru”, built on 1963 at the Mitsubishi shipyard in Japan, was the first ship equipped with a bulbous bow. The ship attained the speed of 20 knots with 13.500 hp while similar ships needed 17.500 hp to reach the same speed.

Here below we can see the Diagram that relates the evolution of the application of bulbs as a function of the Reynolds Number, along the XX century, where we can note that evolution reached different types of vessels and become very useful for now ships at different scales.

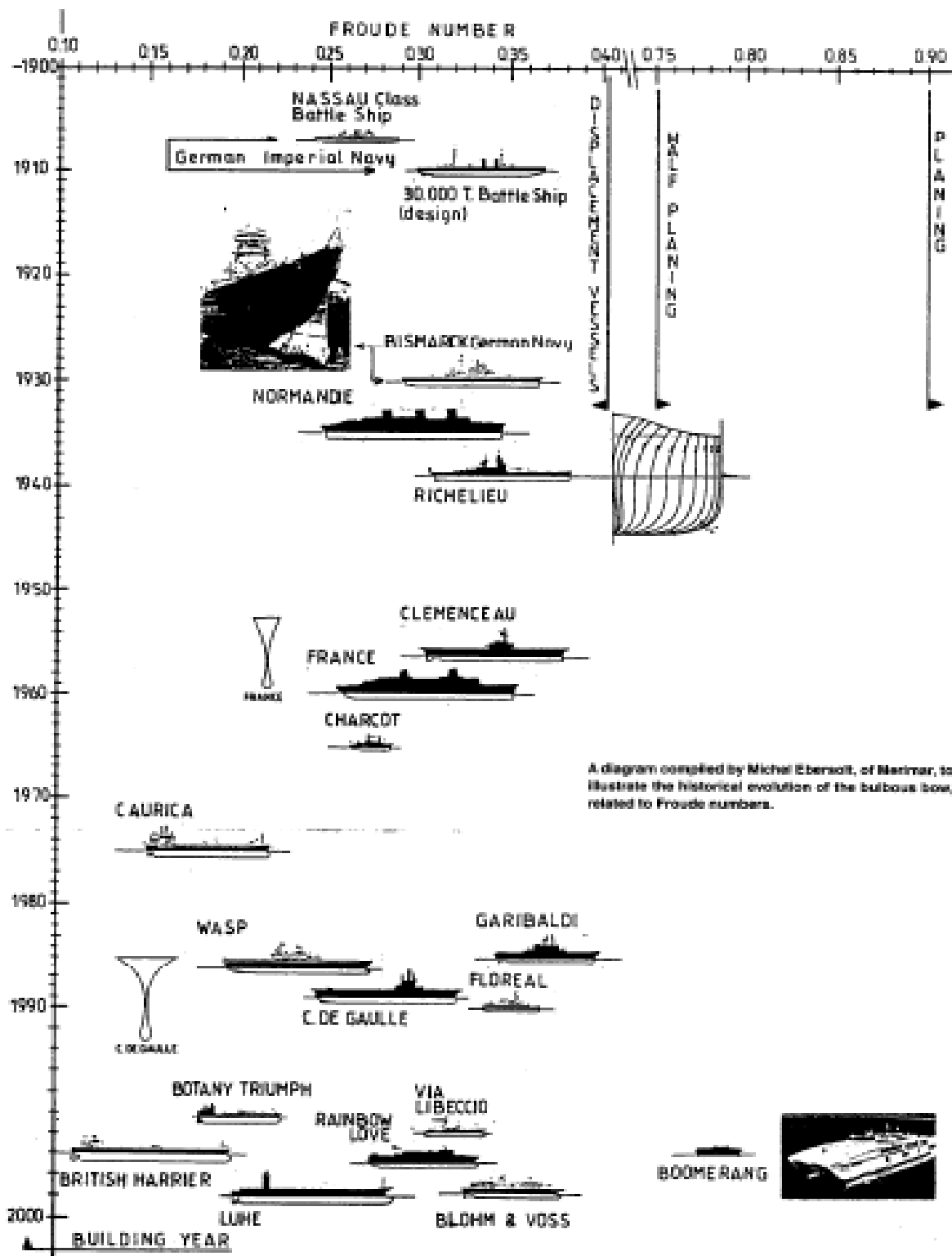


Figure 1: Diagram that relates the evolution of the application of bulbs as a function of the Froude Number, along the XX century

### 1.3 State of Art

Since optimisation methods became a very useful tool in design stage, there are a lot work done on this subject differing from the method used on creating the design individuals as example by parametric method which consist to make some functions to characterize the shape of hull shape, for this there were in 2001, S. Harries & al worked on a parametric modeling approach to the design of ship hull forms which allowed to create and vary ship hulls quickly and efficiently [1]. Also making modification just in a part of it as sectional area curve (SAC), Francisco Perez & al in 2006 who worked on showing the importance of the sectional area curve SAC in the design of a bulbous bow [2].

For the used CFD code, we can note using two main methods potential flow as done by Zhang Bao-Ji in 2009 worked on bow body modification with Rankine source method [3], or a viscous flow like Shahid Mahmood & al in 2012 used fluent as CFD code [4]. Also there is who made a combination as George Tzabiras & al that had developed an integrated hybrid potential-viscous flow method to calculate the total resistance in 2009 [5].

About the optimisation tools ,there are different methods can be used to converge towards the best possible design, as example a genetic algorithm used to evaluate the objectives and introduce new designs in the optimization loop used by Mahmoud & al [4].

The development of this project will be following the below stages:

- 1- Working with a preliminary design to determine the characteristics of the baseline design before application of any changes ,this includes calculation of the drag resistance , checking the wave field around the hull and also some informations related to heave and pitch motion. Since STAR-CCM + ,the CFD code is able to define them with some reliable insurtitises . so this data about the baseline design will be our reference checking criteria.
- 2- Moving for next stage including applying the CFD viscous calculations on designs with modified bow shapes ,bulbous bow adapted by VSP CAD open sources software working with a the parametric method ,this depends on the parameters which introduced to define the bulbous as thinkness , length and breadth.

## Chapter 2

### Theoretical Background

#### 2.1 Bulb forms

Today bulbous forms tapering sharply underneath are preferred, since these reduce slamming. The lower waterplanes also taper sharply, so that for the vessel in ballast the bulb has the same effect as a normal bow lengthened. This avoids additional resistance and spray formation created by the partially submerged bulb. Bulbs with circular cross-sections are preferred where a simple building procedure is required and the potential danger of slamming effects can be avoided. The optimum relation of the forward section shape to the bulb is usually determined by trial and error in computer simulations, for example, Hoyle et al. (1986). Modern bulbous forms, wedge shaped below and projecting in front of the perpendicular, are geometrically particularly well suited to V section forms.

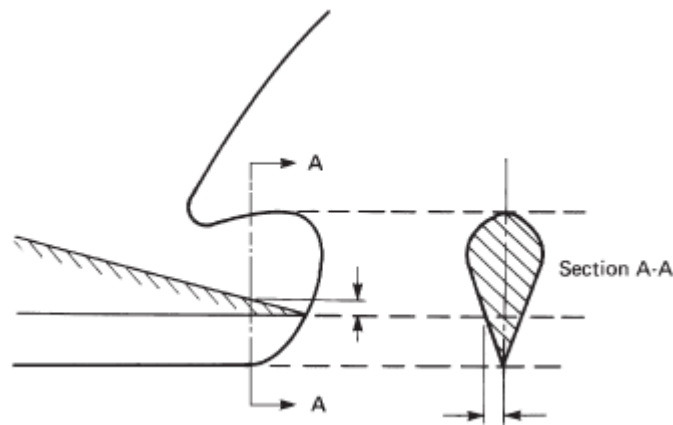


Figure 2 : Modern bulb shapes

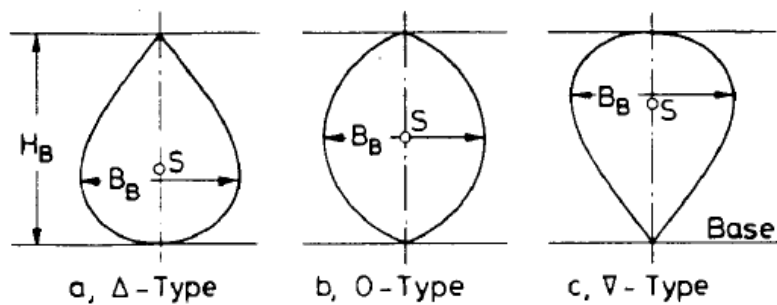


Figure 3 : Bulb types [6]



### 2.1.1 Bulbous bow projecting above CWL

It is often necessary to reduce the resistance caused by the upper side of bulbous bows which project above the CWL creating strong turbulence. The aim should be a fin effect where the upper surface of the bulb runs downwards towards the perpendicular. A bulbous bow projecting above the waterline usually has considerably greater influence on propulsion power requirements than a submerged bulb. Where a bulbous bow projects above the CWL, the authorities may stipulate that the forward perpendicular be taken as the point of intersection of the bulb contour with the CWL. Unlike well-submerged bulbs, this type of bulb form can thus increase the calculation length for freeboard and classification.

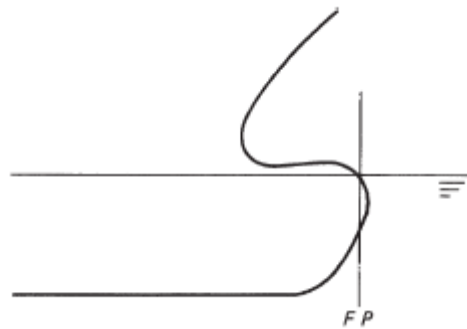


Figure 4: Position of forward perpendicular with high bulbous bows

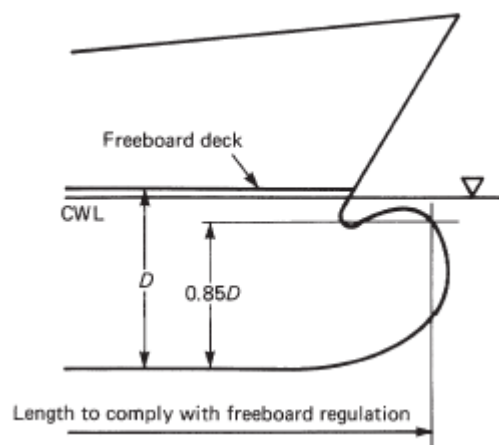


Figure 5: Length of freeboard calculation with low freeboard deck

### **2.1.2 Projecting length:**

The length projecting beyond the forward perpendicular depends on the bulb form and the Froude number. For safety reasons, the bulbous bow is never allowed to project longitudinally beyond the upper end of the stem: 20% B is a favourable size for the projection length. Enlarging this size improves the resistance only negligibly. Today, bulbs are rarely constructed without a projecting length. If the recess in the CWL is filled in, possibly by designing a straight stem line running from the forward edge of the bulb to the upper edge of the stem, the resistance can usually be greatly reduced. This method is hardly ever used.

### **2.1.3 Bulb axis**

The bulb axis is not precisely defined. It should slope downwards toward the stern so as to lie in the flow lines. This criterion is also valid for the line of the maximum bulb breadth and for any concave parts which may be incorporated in the bulb. The inclination of the flow lines directly behind the stem is more pronounced in full than fine vessels. Hence on full ships, the concave part between bulb and hull should incline more steeply towards the stern.

### **2.1.4 Area ratio**

The area ratio  $ABT=AM$  is the ratio of the bulb area at the forward perpendicular to the midship section area. If the bulb just reaches the forward perpendicular, or the forward edge of the bulb is situated behind the forward perpendicular the lines are faired by plotting against the curvature of the section area curve to the perpendicular. At the design draught, the resistance of the ship with deeply submerged bulb decreases with increasing area ratio. A reduction of the area ratio (well below the resistance optimum) can, however, be advocated in the light of the following aspects:

1. Avoidance of excessive slamming effects.
2. The ability to perform anchoring operations without the anchor touching the bulb.
3. Too great a width may increase the resistance of high bulbs, since these are particularly exposed to turbulence in the upper area.

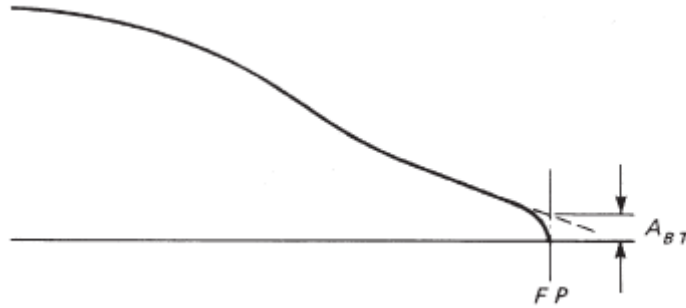


Figure 6: Bulb with projecting length. Theoretical bulb section area of the forward perpendicular

The effective area ratio can be further increased if the bulb is allowed to project above the CWL. Although the section above the CWL is not included in the normal evaluation of the area ratio, it increases the effective area ratio and can considerably reduce resistance, provided that the bulb is of suitable shape.

### 2.1.5 Transition

The transition from a bulbous bow to the hull can be either faired or be discontinuous (superimposed bulb). The faired-in form usually has lower resistance. The more the hollow surface lies in the flowlines, the less it increases resistance. In general, concave surfaces increase resistance less. [6]

## 2.2 Power requirements with bulbous bow

The change in power requirement with the bulbous bow as opposed to the 'normal' bow can be attributed to the following:

- ❖ Change in the pressure drag due to the displacing effect of the bulb and the fin effect.

The bulb has an upper part which acts like a fin. This fin-action is used by the 'stream-flow bulb' to give the sternward flow a downward component, thus diminishing the bow wave. Where the upper side of the bulb rises towards the stem, however, the fin effect decreases this resistance advantage. Since a fin effect can hardly be avoided, care should be taken that the effect works in the right direction. Surprisingly little use is made of this resistance reduction method.

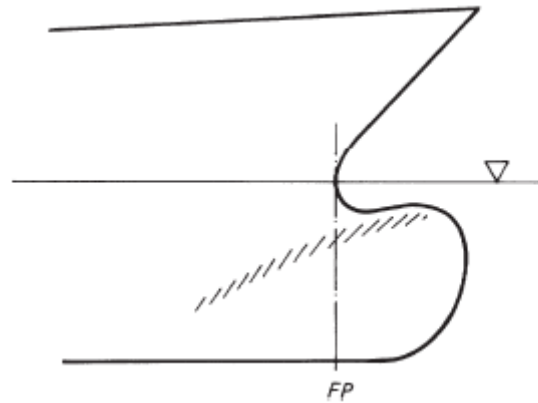


Figure 7: Fin bulb

- ❖ Change in wave breaking resistance.

With or without bulb, spray can form at the bow. By shaping the bow suitably (e.g. with sharply tapering waterlines and steep sections), spray can be reduced or completely eliminated.

- ❖ Increase in frictional resistance.

The increased area of the wetted surface increases the frictional resistance. At low speeds, this increase is usually greater than the reduction in resistance caused by other factors.

- ❖ Change in energy of the vortices originating at the bow.

A vortex is created because the lateral acceleration of the water in the CWL area of the fore body is greater than it is below. The separation of vortices is sometimes seen at the bilge in the area of the forward shoulder. The bulbous bow can be used to change these vortices. This may reduce energy losses due to these vortices and affect also the degree of energy recovery by the propeller (Hoekstra, 1975).

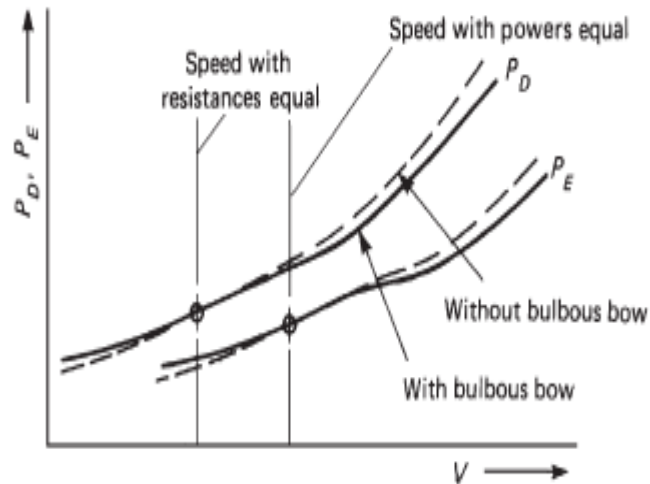


Figure 8: Resistance comparison (ship with and without bulbous bow)

The power savings by a bulbous bow may, depending on the shape of the bulb, increase or decrease with a reduction in draught. The lower sections of modern bulbous bows often taper sharply. [7]

### 2.3 Parametric ship design

Parametric ship design hull has been as a powerful modeling technique during the last decade. Instead of describing the hull shape's properties by a large network of lines and points requiring a lot of manual work, the parametric modelling approach employs so-called high-level form descriptors which describe characteristic properties, e.g. of the sections by means of longitudinal distributions. There is a preferred technique builds B-spline curves from selected properties. These can be described directly, differentially or even by integral formulations. The vertices of the final spline are then automatically placed to ensure a fair distribution of the property required. A typical example is the sectional area curve of a hull where the integral value reflects the required buoyancy. Direct parameters are derived from the main section geometry and a differential parameter is required at the main section location. The generation of such 'meta curves' is set up in a way that additional constraints may be added later while missing information is found automatically by an internal optimization focusing on maximum fairness, Harries (1999).

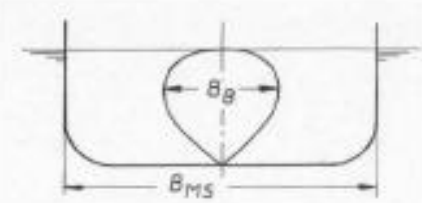
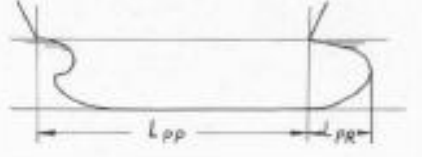
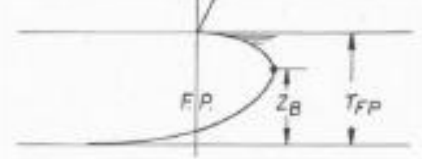
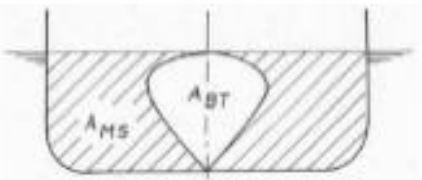
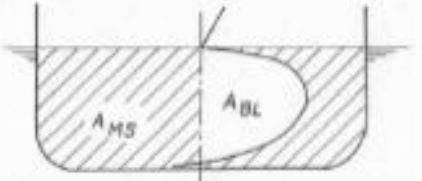

Breadth parameter	$c_{BB} = \frac{B_B}{B_{MS}}$	
Length parameter	$c_{LPR} = \frac{L_{PR}}{L_{PP}}$	
Depth parameter	$c_{ZB} = \frac{z_B}{T_{FP}}$	
Cross area parameter	$c_{ABT} = \frac{A_{BT}}{A_{MS}}$	
Length area parameter	$c_{ABL} = \frac{A_{BL}}{A_{MS}}$	
Volumetric parameter	$c_{\nabla PR} = \frac{\nabla_{PR}}{\nabla_{WL}}$	

Figure 9: Dimensionless bulbous bow parameters as defined by Kracht

### 2.3.1 Parameters of design:

For this project, parameters used for creations of designs for the optimisation will focused on three different parameters related to the length ,breadth and the height of bulbous , in order to create such domain of design experiments shown in figure 10,but in this case we don't know where it will be the optimal design.

## Hydrodynamic optimisation of new hull bow shape by CFD code

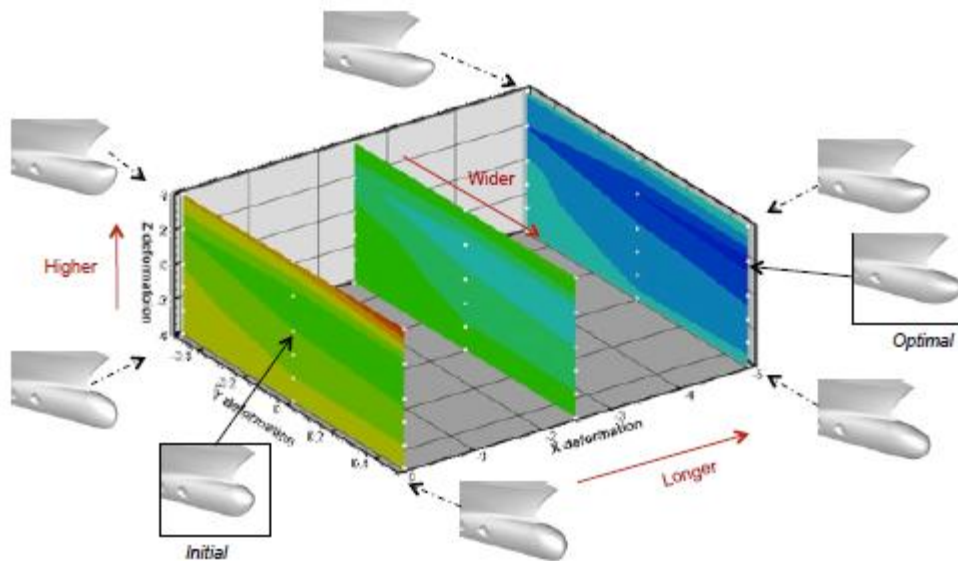


Figure 10 : Parameters of optimisation of bulbous [8]

# Chapter 3

## Principles of CFD

---

### 3.1 Resistance Calculation with RANS CFD Methods

The application of Computational Fluid Dynamics (CFD) by means of solving the Reynolds-Averaged Navier Stokes Equations by numerical means has become an important component of the available tools for solving ship hydrodynamics problems. Specifically, their application to the prediction of ship resistance, including relevant basic principles which apply to other application fields too. The reports from the resistance committee of the ITTC conferences show the advances of CFD in resistance prediction over the last decades, being the increased presence of RANSE CFD since the beginning of the nineties evident.

Another important mirror of the developments of each period has been the CFD workshops created in 1994 in Tokyo (Japan) or in Gothenburg (Germany) in 2000. Beginning from simple applications solving single-phase fluid problems without turbulence, the application of turbulence models in the beginnings of the nineties were an important step for further, more realistic applications in ship hydrodynamics. At that time, an important trend could be observed: the prevalence of finite volume methods compared to finite differences and finite element methods. Later on, the development of free surface techniques could be observed, the techniques of Volume of Fluid, Level Set and Surface Tracking becoming the most widespread for this purpose. Later developments for unsteady simulations, grid motion and further advances in numerical and physical modeling, hand in hand with the ceaseless development of hardware and massive parallelization make the future of RANSE CFD even more promising.

### 3.2 Governing equations

The number of governing equations depends of the problem to be solved, and considering that a continuum mechanics problem is handled here, mass and momentum conservation are always present. Thermal and/or chemical energy balance and additional scalar transport equations such as turbulent kinetic energy or phase fraction (e.g. in the Volume of Fluid Method) are typical exponents of additional transport equations which are usually solved together with the basic conservation equations.



For mass conservation:

$$\frac{\partial \rho}{\partial t} + \nabla \cdot (\rho \vec{u}) = 0$$

and for momentum conservation:

$$\rho \left( \frac{\partial (\vec{u})}{\partial t} + (\vec{u} \cdot \nabla) \vec{u} \right) = f - \nabla p + \nabla T$$

where f is body forces (e.g. gravitation, Coriolis force, etc.) and T is the stress tensor defined by:

$$T = \mu \left( \nabla \vec{u} + \left( \overline{\nabla \vec{u}} \right)^T - \frac{2}{3} (\nabla \cdot \vec{u}) I \right)$$

where I represents a 3x3 identity matrix. For an incompressible flow, the stress tensor can be simplified, leading to:

$$\rho \left( \frac{\partial (\vec{u})}{\partial t} + (\vec{u} \cdot \nabla) \vec{u} \right) = f - \nabla p + \mu \nabla^2 \vec{u}$$

For engineering problems, the application of the Reynolds Averaged Navier-Stokes Equations for turbulent flows represent a good trade-off between computational effort and quality of the results. In this approach, the small scales of the unsteadiness of the flow are averaged (by means of time averaging for statistically steady flows or ensemble averaging for unsteady flows), permitting the solution of the problem with a much larger spatial and temporal discretization as when turbulence is calculated totally (e.g. direct numerical simulations, DNS) or partially (e.g. large eddy simulations, LES) with numerical methods. Due to the non-linearity of the Navier-Stokes equation, time-averaging causes the appearance of an additional term, the Reynolds stress tensor R writing for the RANS equations:

$$\rho \left( \frac{\partial(\bar{\mathbf{u}})}{\partial t} + (\bar{\mathbf{u}} \cdot \nabla) \bar{\mathbf{u}} \right) = -\nabla \bar{p} + \mu \nabla^2 \bar{\mathbf{u}} + \mathbf{f} - \nabla R$$

With R (in index notation):

$$R_{ij} = \overline{\rho u'_i u'_j}$$

Considering  $\bar{\mathbf{u}}$  as the average velocity and  $\bar{u}'$  is the fluctuation of it. Since the equation is not closed anymore, the Reynolds stress tensor must be modeled by means of a turbulence model. For ship hydrodynamics problems, two-equation turbulence models are the most widespread ones and, among these, to mention but some of them, the  $k - \varepsilon$ , the  $k - \omega$  and the  $k - \omega$ -SST models are quite popular ones. A common characteristic of the mentioned models is that the Reynolds stresses are collected into the shear stress term  $\mu \nabla^2 \bar{\mathbf{u}}$  by means of replacing  $\mu$  by the effective viscosity  $\mu_{eff} = \mu + \mu_t$ . Each of the mentioned models applies a different approach for the estimation of the turbulent viscosity  $\mu_t$ .

An additional matter of interest for ship hydrodynamic problems is the treatment of the free surface. A widespread method, which has also been applied in this investigation work, is the Volume of Fluid method (VOF). This methodology, an interface capturing method, determines the shape of the free surface in a fixed mesh allocating for each cell a scalar quantity, the phase fraction  $\gamma$ , and solving the correspondent transport equation:

$$\frac{\partial \gamma}{\partial t} + \nabla \cdot (\gamma \vec{u}) = 0$$

The phase fraction has a value of  $\gamma = 0$  for total absence of a definite phase in a cell and  $\gamma = 1$  for a completely filled cell. For two-phase problems (in ship hydrodynamics applications normally water and air), the second phase has a phase fraction equal to  $\gamma - 1$

### 3.3 Turbulent boundary layer

Since we are dealing with high Reynolds number due to working with resistance computation on full scale model, it is necessary to satisfy the condition of wall distance when using prism

layer grid for the calculation near to the wall this can be explained by wall  $y^+$  distance to estimate the distance of the layer of the grid should be satisfied:

$$y^+ = \frac{y \cdot u_t}{\nu} \quad , \quad u_t = \sqrt{\frac{\tau_w}{\rho}} \quad \text{and} \quad u^+ = \frac{u}{u_t}$$

Where:

$y^+$  : Wall coordinate

$y$  : Distance  $y$  to the wall

$u^+$  : Dimensionless velocity

$u$  : Velocity parallel to the wall

$\tau_w$  : Wall shear stress

$u_t$  : Friction velocity or shear velocity

### 3.4 Courant number

It is known that Courant number depends on velocity, cell-size and time step and it is calculated for each cell, the Courant number will change according to velocity when we use a fixed time step under the formula below:

$$Co = \frac{\Delta t \cdot u}{\Delta x}$$

Where:

$\Delta x$  : Dimensional interval

$\Delta t$  : Time interval

$u$  : Speed in the X direction

The physical explanation of this number in CFD simulation is that the Courant number can tell us about the movement of fluid through the computational grid cells, so if  $Co \leq 1$  that means the fluid particle is moving from one cell to another within one time step (at most) while if  $Co$  is bigger than 1 that means the fluid particle is moving more than one cell per one time cell which can occur a negative convergence.

## Chapter 4

# Resistance computation on STAR-CCM+

---

### 4.1 Resistance of bear hull

This project is dealing with a military frigate with 75m of length design; this kind of ships is basically more focused on maximum speed of 25knots.

Here below this table is showing main dimensions and data used to do the simulation tests on this ship:

Dimensions of the ship	symboles	value	units(SI)
Length over all	LOA	75.78	m
Length at Water line	LWL	69.92	m
Maximum breadth	BOA	10.57	m
Breadth at water line	BWL	9.97	m
Draft	T	2.9	m
Volume	$\nabla$	953.7	m <sup>3</sup>
Weight	$\Delta$	977.5	ton

Table 1 Main Dimensions and data of the ship

For the center of gravity used to set the motions references:

LCG= 32.044m from Transom

TCG = 0.00 m from CL

VCG = 4.604 m from BL

For motions calculation by Star ccm+, it is needed to use some approximation to get data for inertia to use them for calculation trim and heave motions:

$$I_{xG} = \Delta_m \cdot k_{xG}^2$$

$$I_{yG} = I_{zG} = \Delta_m \cdot k_{yG}^2$$

With:  $\Delta_m = \rho V$  ,  $k_{xG} \approx 0.40B$  and  $k_{yG} = k_{zG} \approx 0.26L$

Where:  $k_{xG}$  and  $k_{yG}$  is radius of gyration about center of gravity G

## Hydrodynamic optimisation of new hull bow shape by CFD code

$I_{xG}$ ,  $I_{yG}$  and  $I_{zG}$  are moments of inertia around x, y and z respectively.

$\Delta_m$ : Displacement,  $V$ : volume,  $\rho$ : density,  $L$ : ship length,  $B$ =ship beam

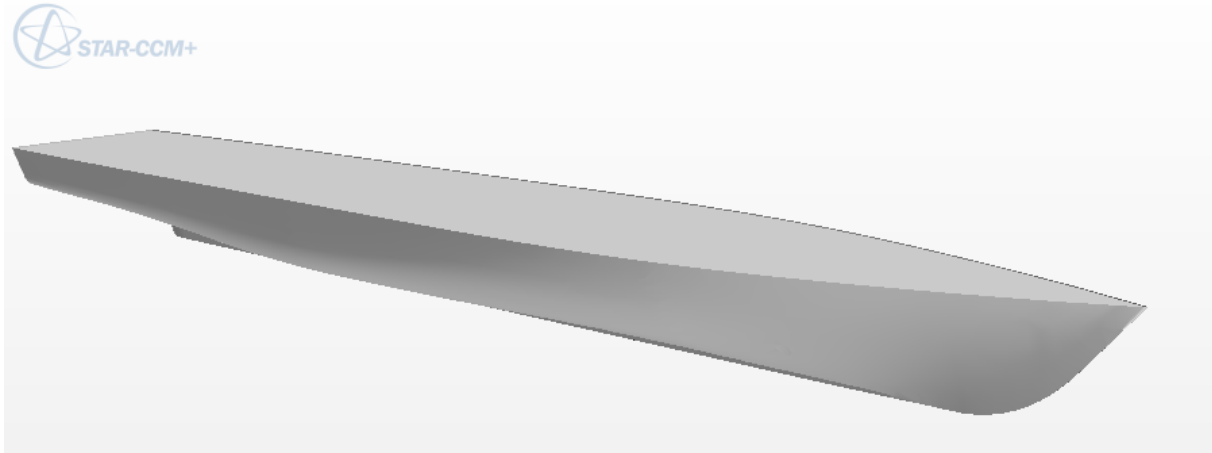


Figure 11: Hull form without bulbous of studied case

### 4.2 Overset mesh

Overset meshes, also known as “Chimera” or overlapping meshes, are used to discretize a computational domain with several different meshes that overlap each other in an arbitrary manner. They are most useful in problems dealing with multiple or moving bodies, as well as optimization studies. In most cases, using overset meshes does not require any mesh modification after generating the initial mesh, thus offering greater flexibility over the standard meshing techniques.

Using an overset mesh requires creating a background region, which is a closed surface solution domain, and one or more overset regions, which contain the physical bodies. More than one overset region can be used on top of the background region, but one overset region cannot overlap with another overset region.

The overset mesh feature is supported for use with the following:

- Segregated and coupled flow
- DFBI
- Motion models and reference frames

- Single phase
- VOF Multiphase
- Lagrangian Multiphase

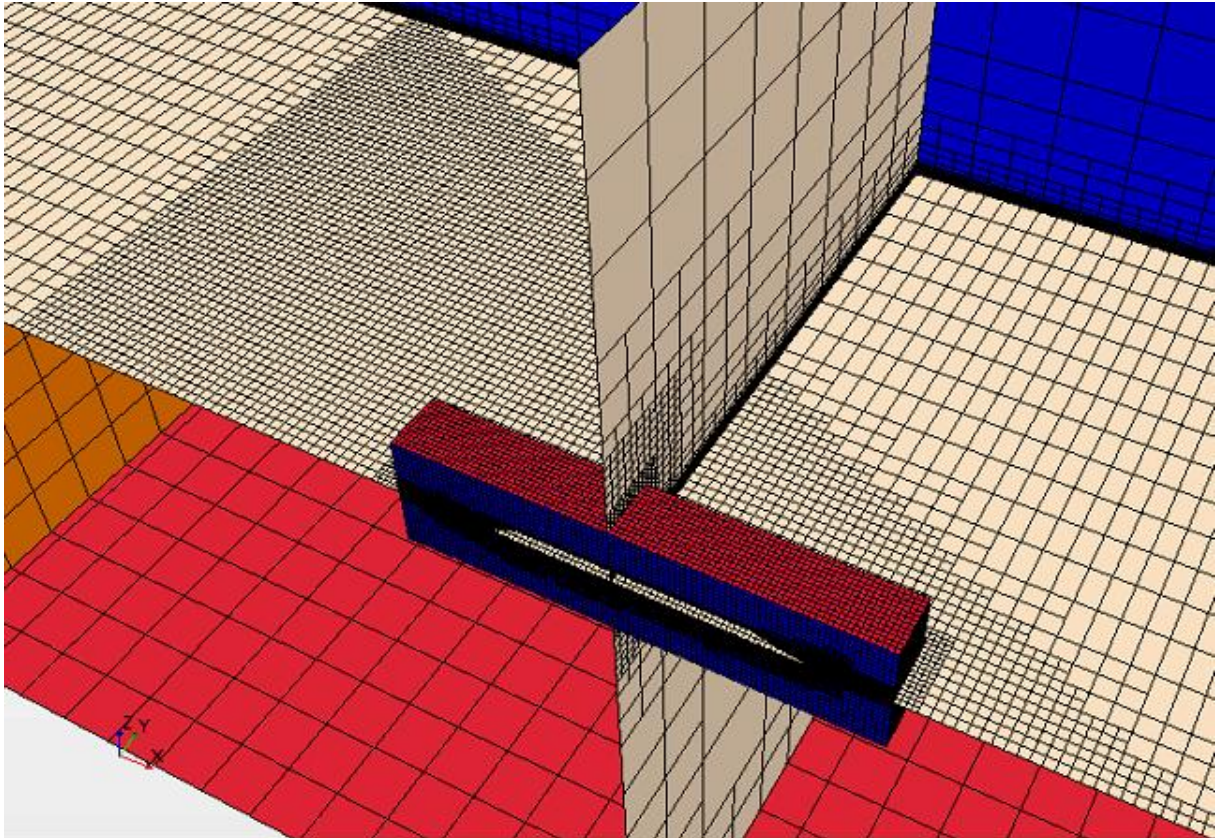


Figure 12: Volume mesh of bare hull on STAR-CCM+

This figure above show the volume mesh of the domain using to main rigion of background and overset region around the ship, considering symmetry, we do apply the computation on just on a half ship as it is case of symmetry and for CFD code to have less number of cells of the grid so less computation time.

Also for the tracking of the wave around the ship, two volume control were used one coarse rectangular covering all the domain length and width of 2.5 m height and another finer meshed triangular volume control for region mostly concerned of wave wake of the ship .

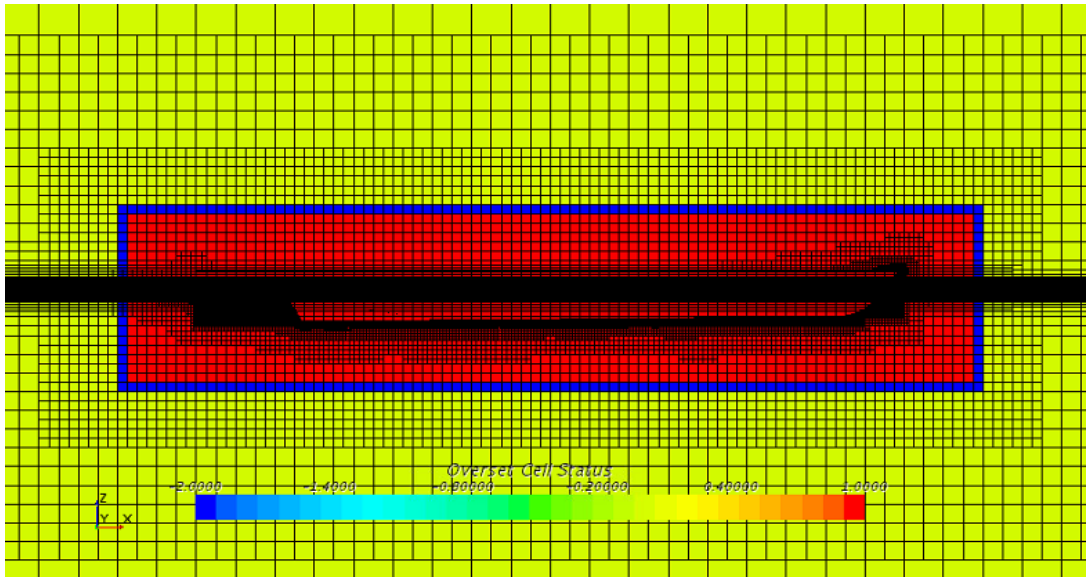


Figure 13: Overset cell status of the background region

The figure shows the overset cell status for the background region, the passive cells are red on the overset region, the active cells are yellow on background region and the acceptor cells are in between of two regions in the overlap region.

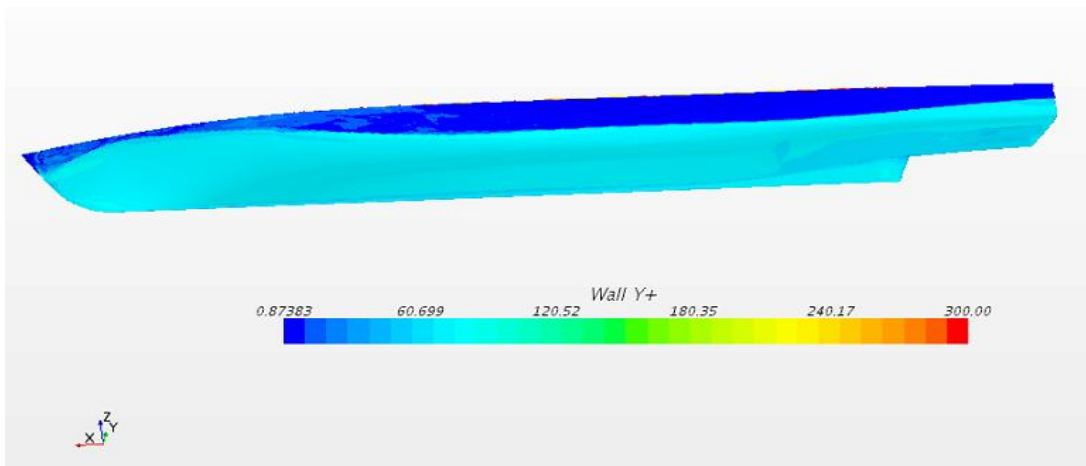


Figure 14: Wall Y+ contour field for wall function

From this figure the wall Y+ conditions is satisfied with criteria that should be in range of  $30 < \text{wall } Y+ < 300$



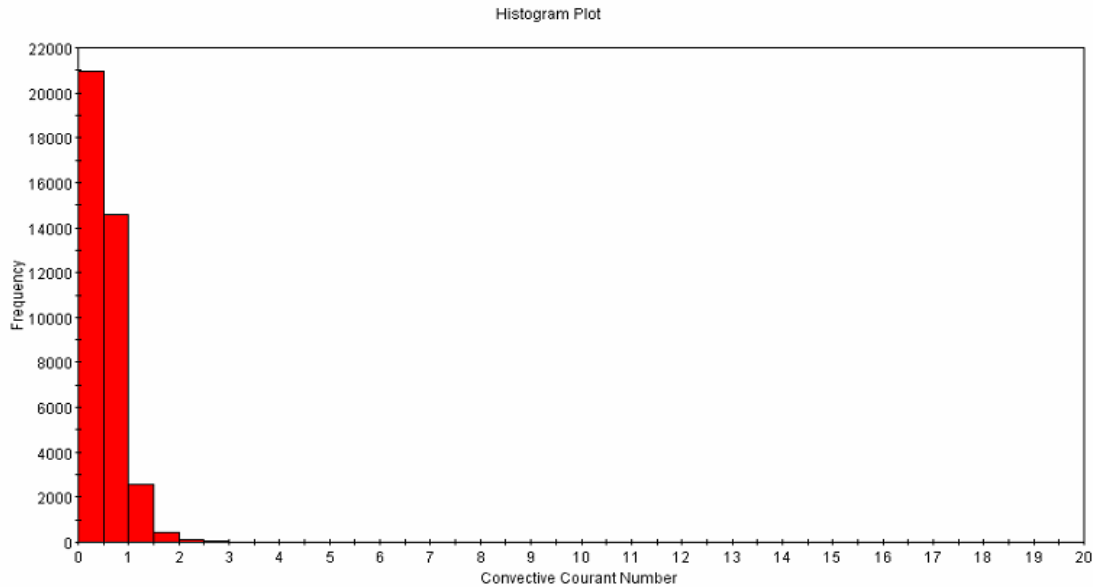


Figure 15: Courant number used in simulations

The histogram of Courant number plotted on the free surface shows that Co number condition was respected and taking time step of 0.004 s was suitable with the use of mesh density of 2.1 millions cells. Most cells have Co number less than 1 and some of them exceed that limit but do not go beyond 5. For this reason we can say that Co is offering a good accuracy for results.

### 4.3 Results for Resistance for three speeds

Before starting doing optimisation on drag reduction of ship resistance, it is required to validate the results got by Star ccm+ using a certain mesh densities and the conditions applied on boundaries and solver by experimental results of towing tank test of the ship.

After that calculation on ship adopting the bulbous bow can be done to see how much gain in drag resistance can be reached with bulbous.

Tests of resistance for the bare hull for different speeds of 15, 20 and 25 knots have been ran for 9 days on a computer of 16 core with mesh density of 2.1 million cells.

Here below, figures showing the development of forces drag and lift acting on the bare hull (half ship) with respect to time and the wave pattern for three cases are also shown :



## Hydrodynamic optimisation of new hull bow shape by CFD code

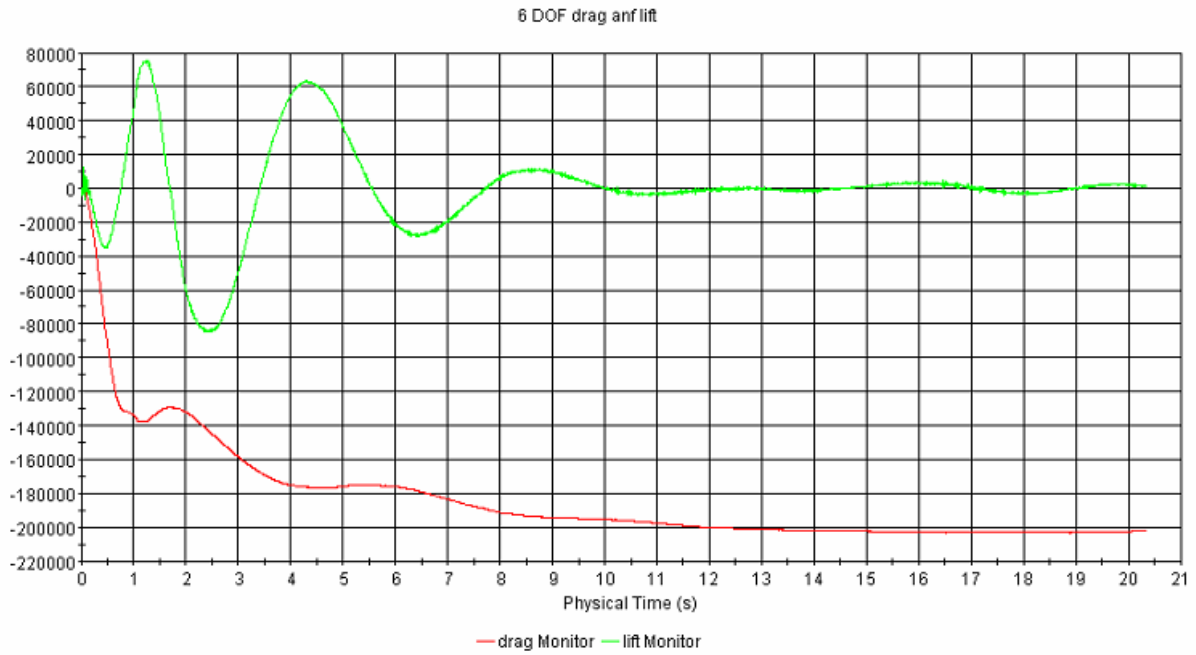


Figure 16: Drag and lift development with respect to time for 25 knots

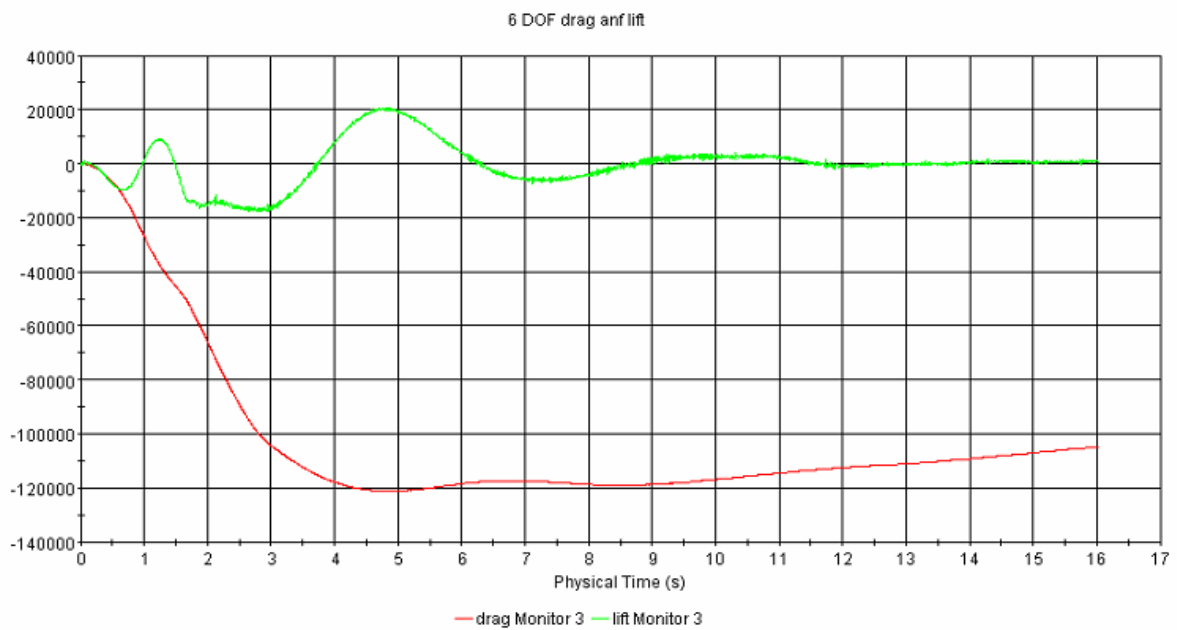


Figure 17: Drag and lift development with respect to time for 20 knots

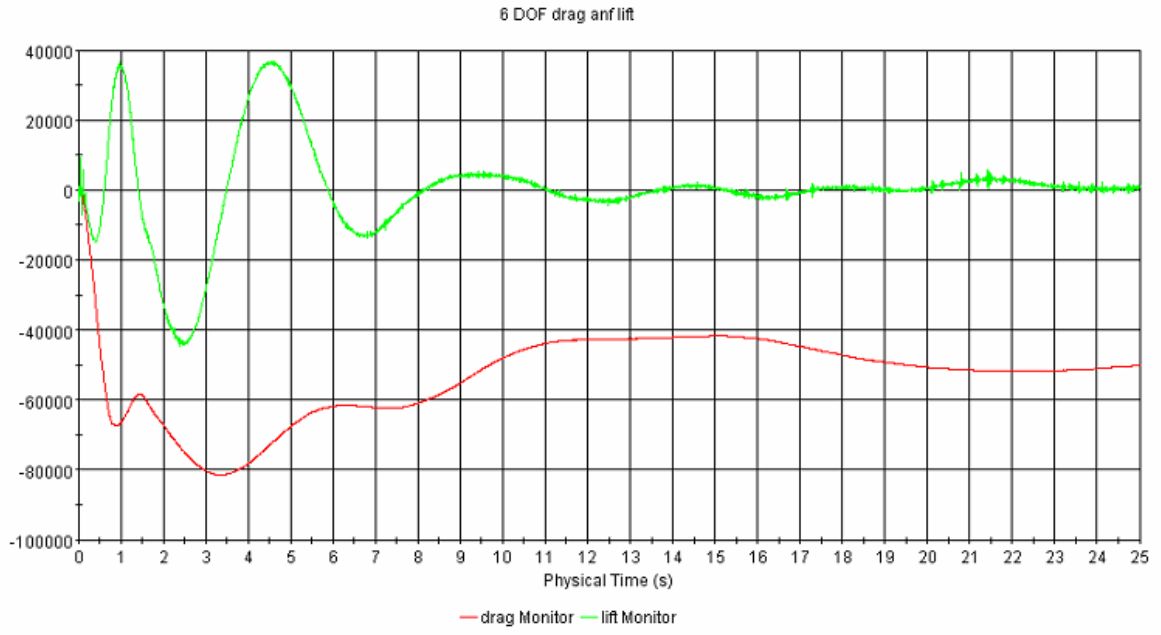


Figure 18: Drag and lift development with respect to time for 15 knots

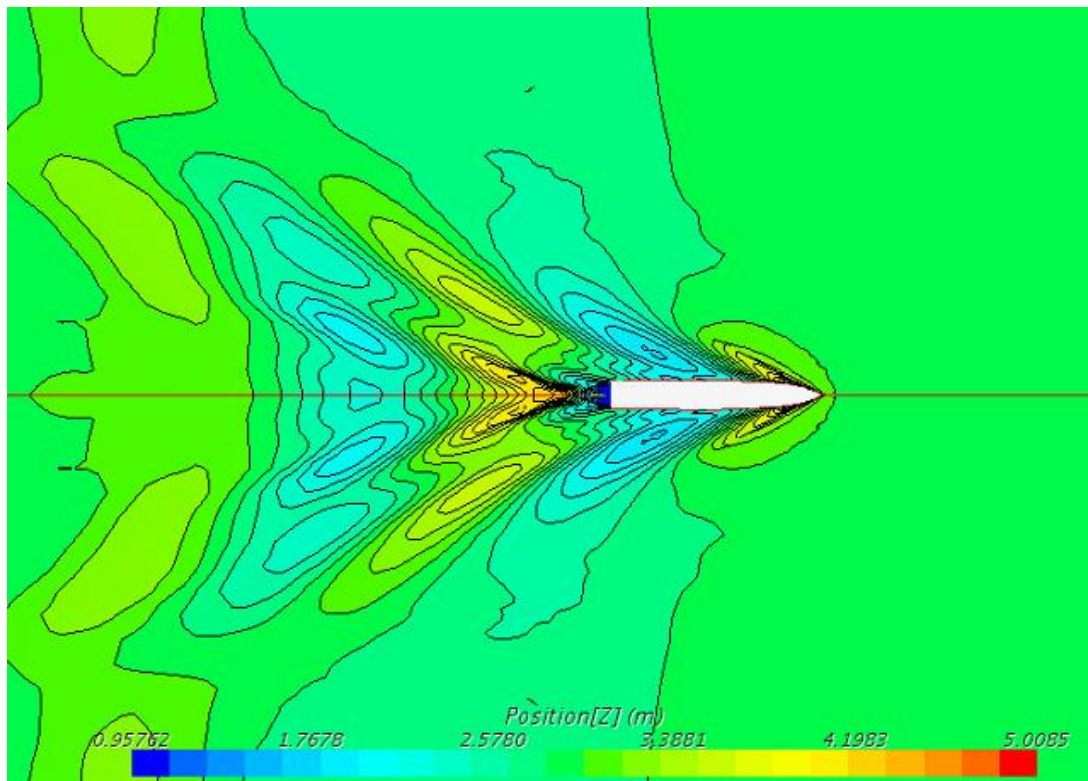


Figure 19: Wave pattern for bare hull for 25 knots

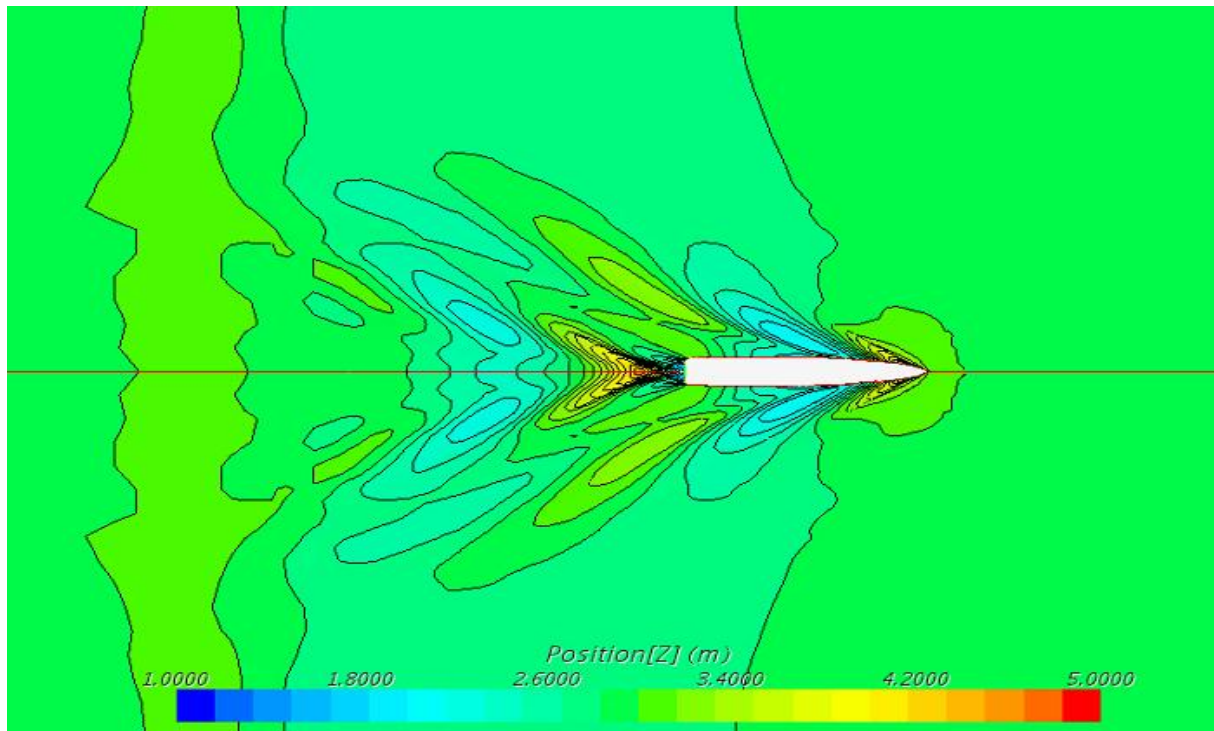


Figure 20: Wave pattern for bare hull for 20 knots

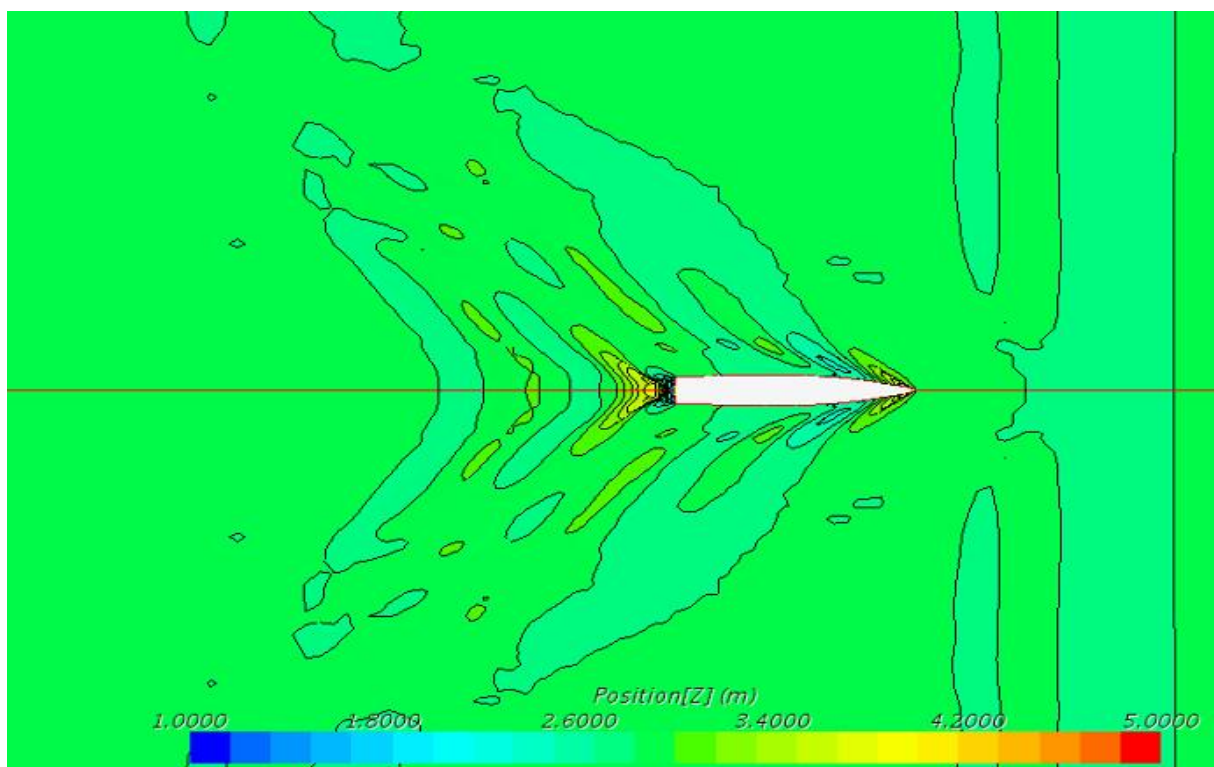


Figure 21: Wave pattern for bare hull for 15 knots

The heave and trim motion are representing in graphs below showing a normal behavior for a semi displacement ship, trim of  $1.14^\circ$  deg and sinkage of 350 mm.

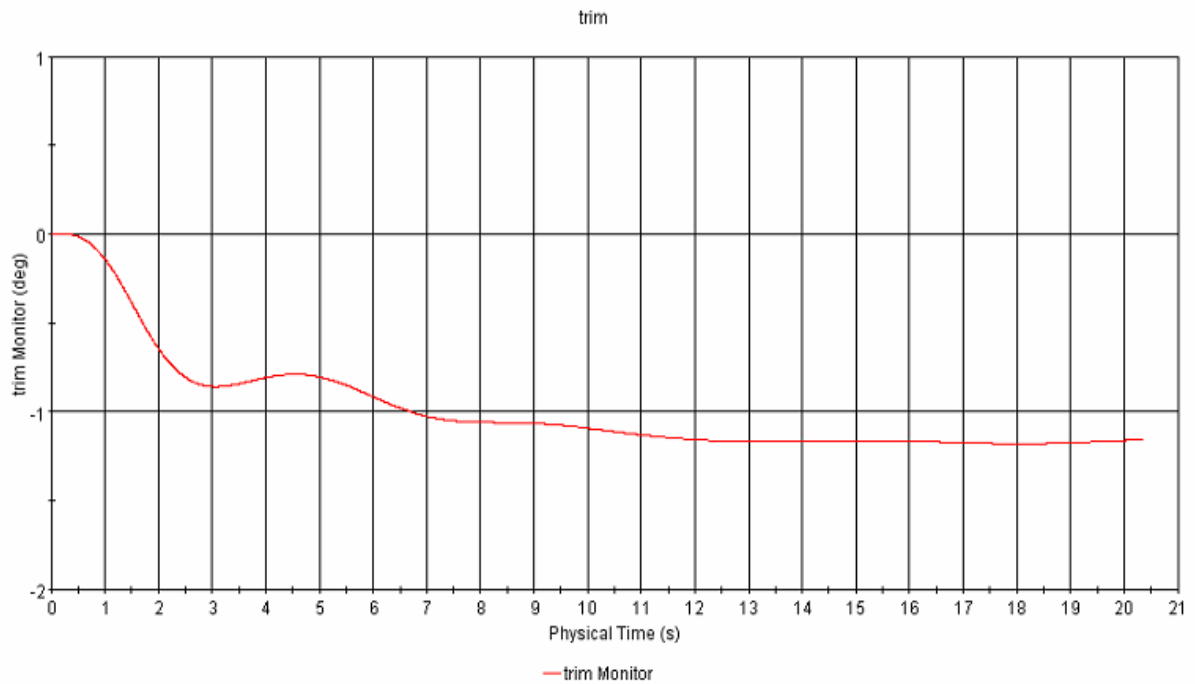


Figure 22: Trim angle for bare hull for 25knots

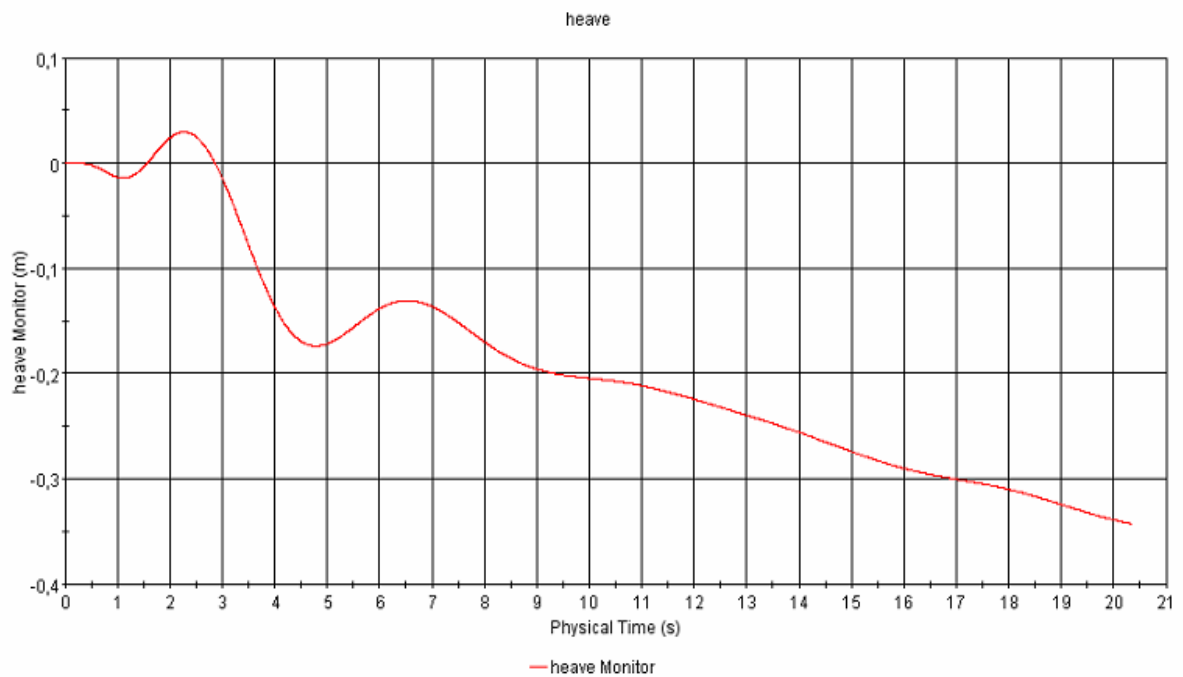


Figure 23: Heave motion for bare hull for 25 knots

#### 4.4 Comparison of resistance results

Results shown before were taken and represented on a graph for purpose of validation.

In below (figure 23), there is two results, numerical of STAR-CCM+ and predicted method of Holtrop Mannen 84.

Instead of experimental results which are not yet performed for this ship, these results are for clean bare hull and not including the appendages (twin screw, bow thrusters and two rudders).

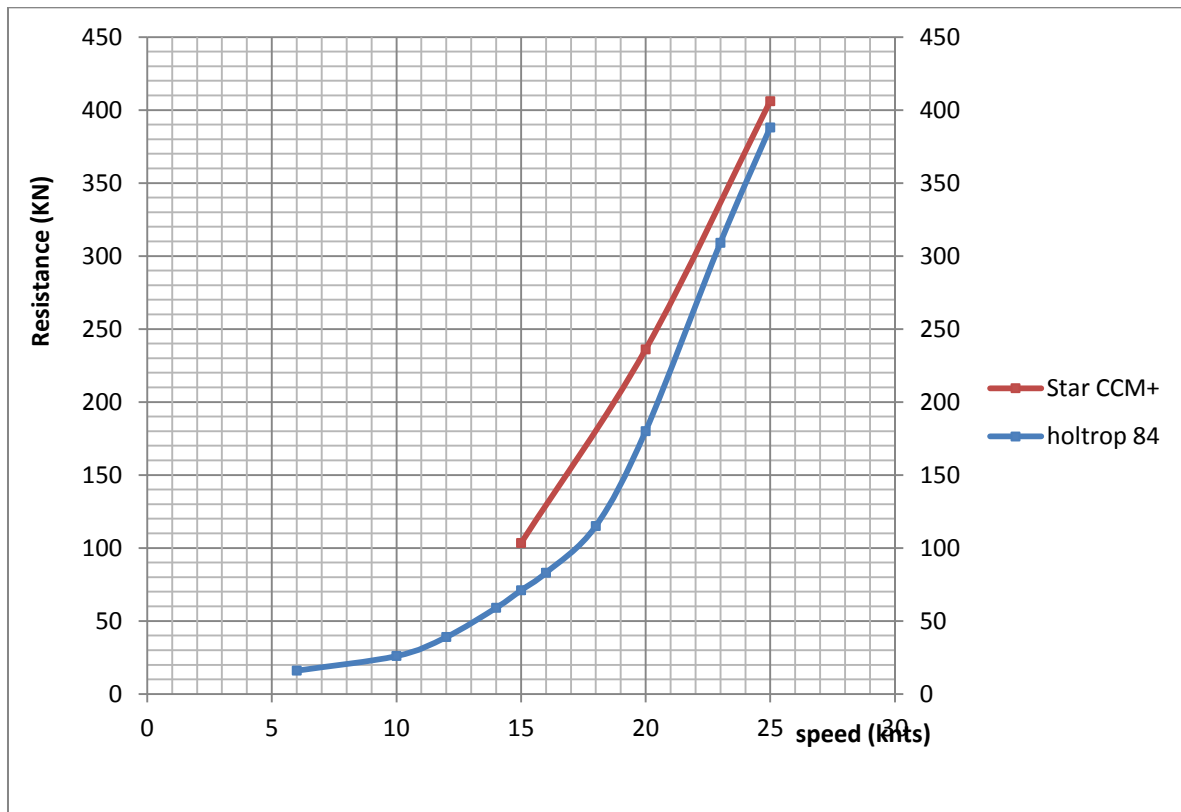


Figure 24: Comparison between results of STAR-CCM+ and Holtrop 84 for bare hull

In addition, there was other prediction methods used for this project as DeGroot method and CRTS method shown in (figure 24). These methods are used for prediction power in sea, (means taking in account the skin roughness of the hull which considered almost 10% with comparison to bare hull resistance. the appendages has been taken in account as resistance value of 40 KN based on experiences of the company with such kind of projects, so adding these two parts of resistance to the total drag got from Star ccm+ results in order to make this comparison.

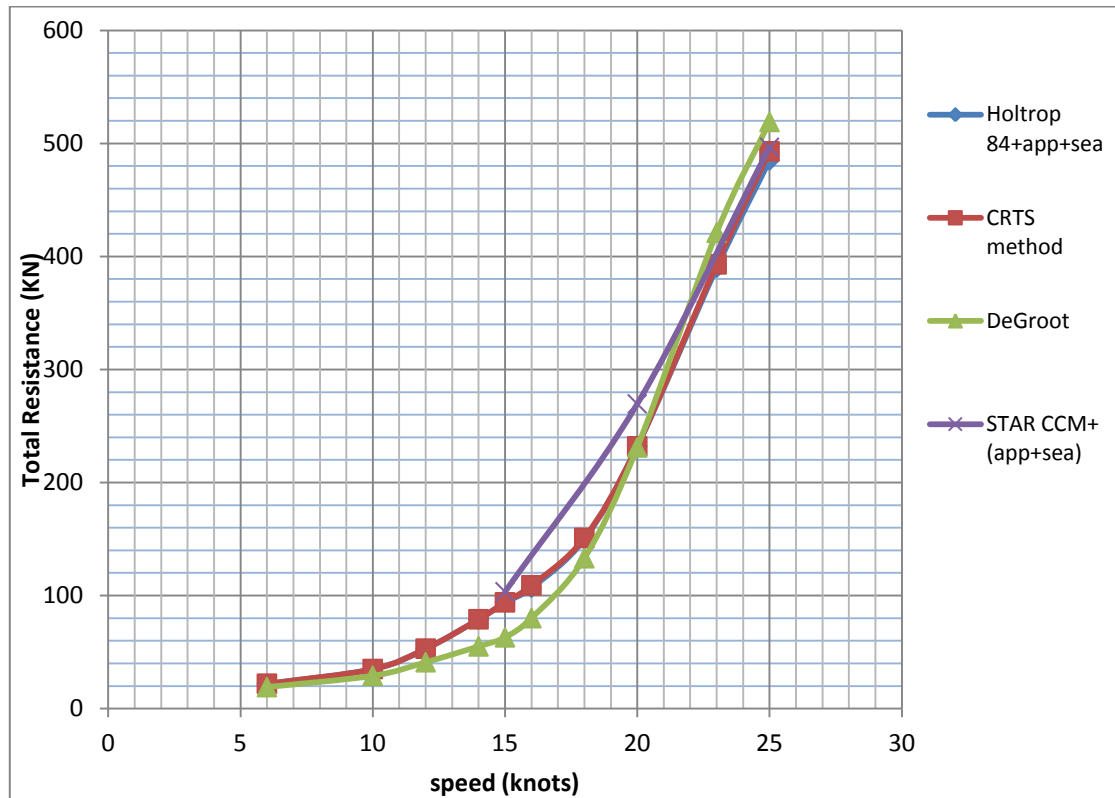


Figure 25: STAR-CCM+ vs different power prediction methods for hull with appendages & hull roughness

We can see a good consistency in results for higher speed for STAR-CCM+ with De Groot and CRTS method by being in range of the two, there is but less accordance for 20 knots. As far we don't have the experimental test results, we can't describe exactly the reason for this difference.

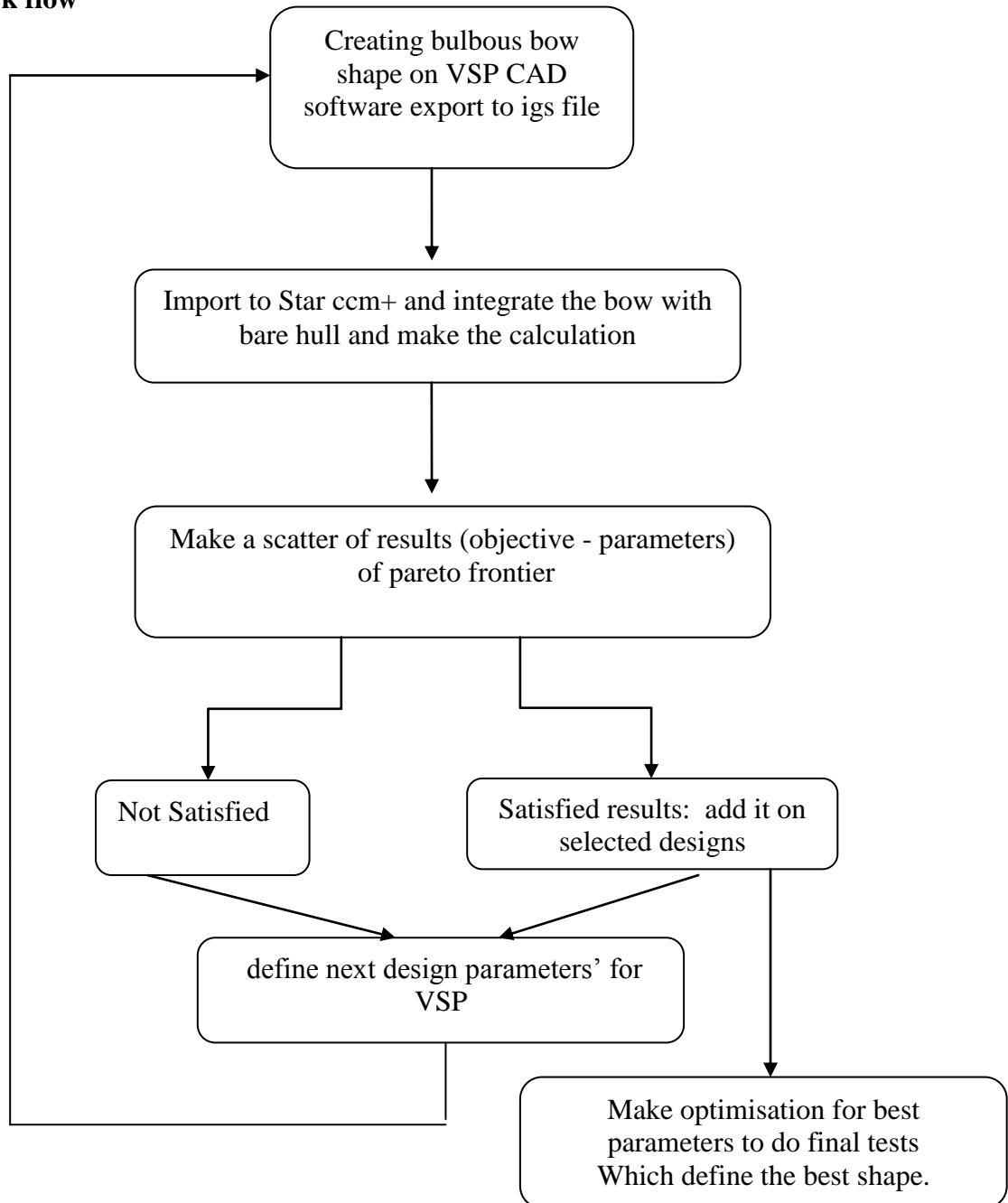
After this checking of STAR-CCM+ results, it is possible now move to calculate drag resistance with bulbous using this setting of mesh and solver parameters' which can be considered as reliable .

## Chapter 5

### Optimisation tests

---

#### 5.1 Work flow



## 5.2 Base design

To start optimisation a bulbous bow for the ship was designed in company. Figure 26 is showing a cut of hull which will be used to build individual designs, the method rely on keeping the section joining between hull and bulbous bow shape fix in order to avoid bringing undesired modifications to hull shape. Then make setting parameters to control the rest part of bulbous.

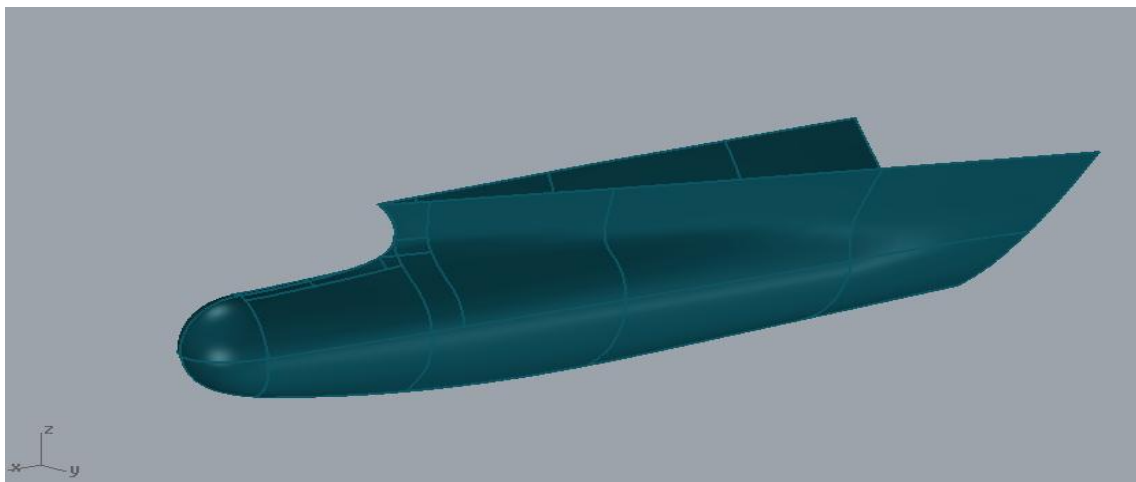


Figure 26: Base design of bulbous bow

And here below the full ship with base bulbous design:

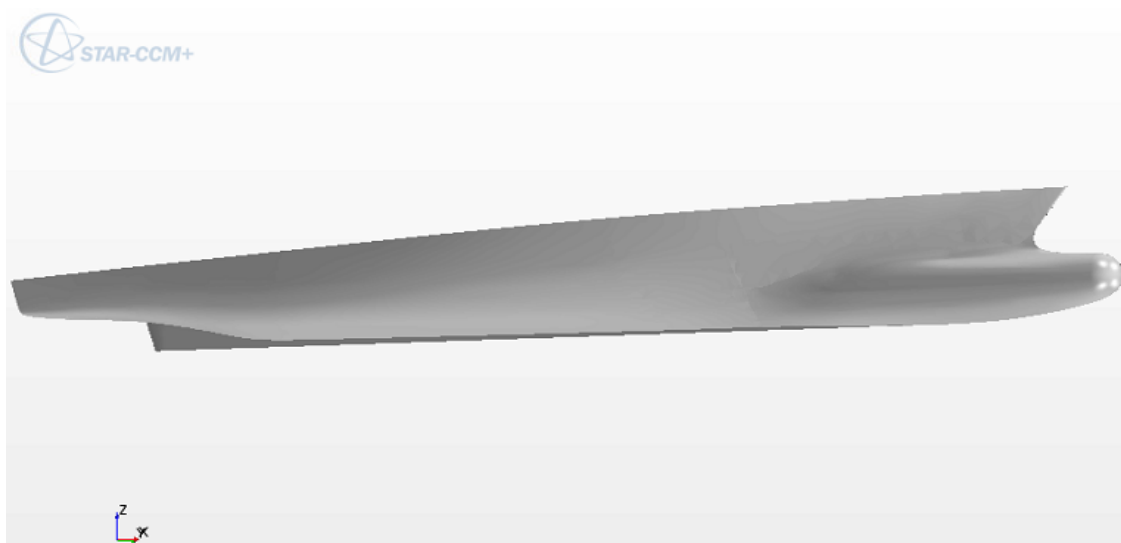


Figure 27: Ship base design



### 5.3 Calculating total resistance of base design

Performing computation on design will increase a bit the number of cells in domain. That is due to need to satisfy a nice mesh around bulb, mesh was increased to 1.2 millions cell

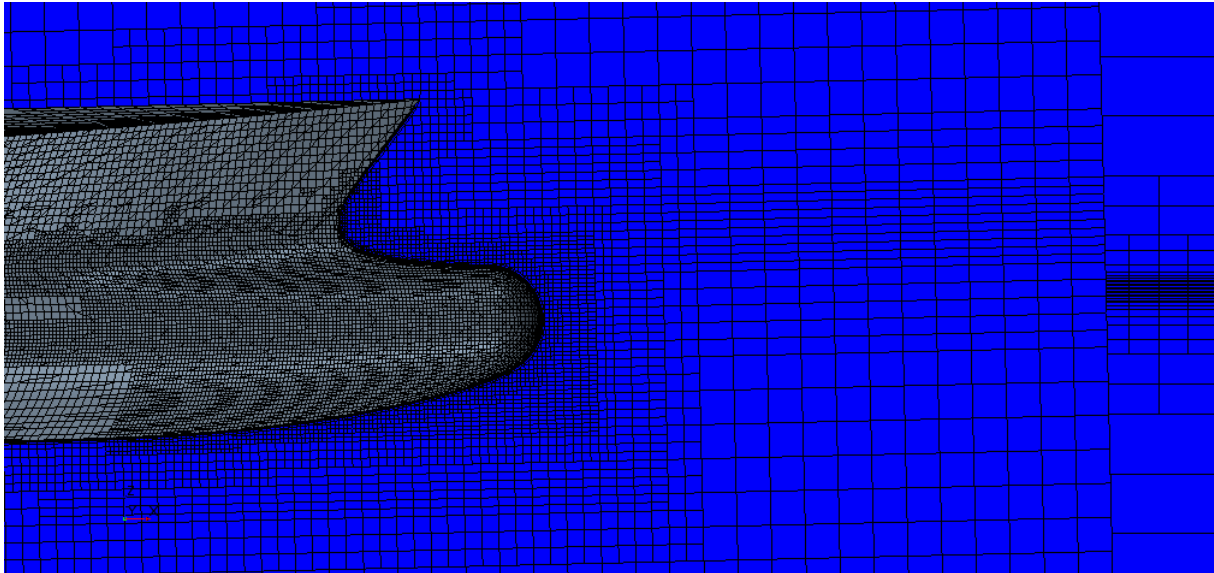


Figure 28: Mesh of base bulbous design

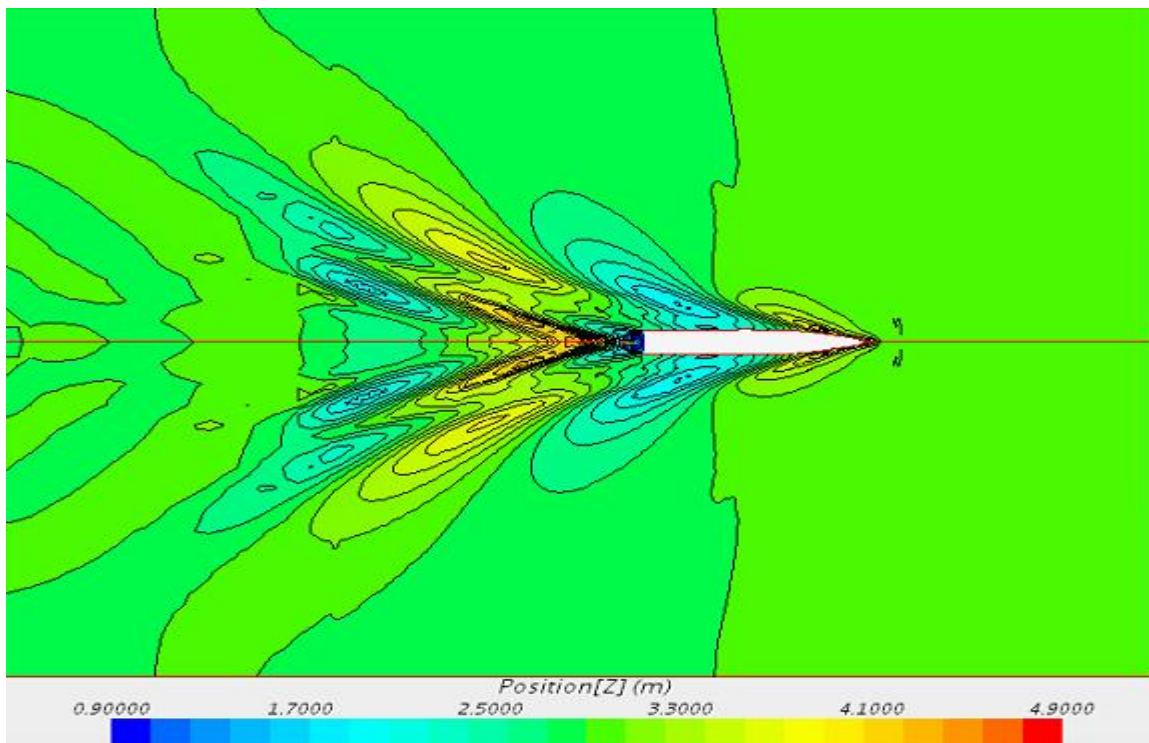


Figure 29: Wave pattern around the ship for base design

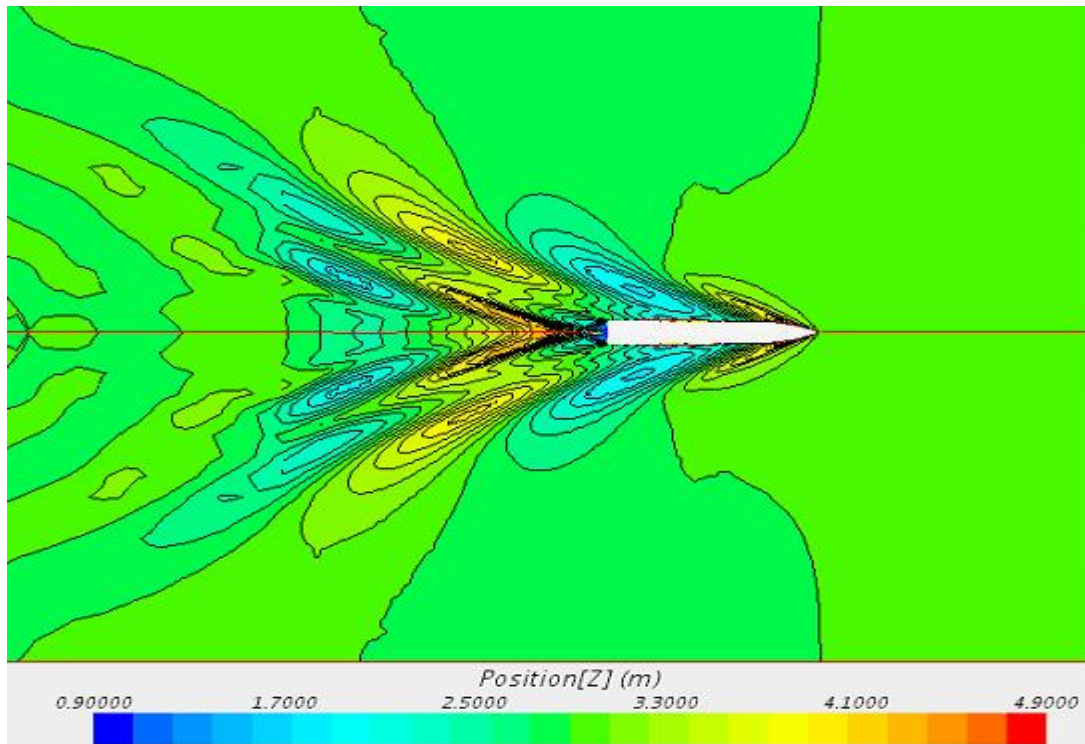


Figure 30: Wave pattern around the bare hull

From both free surface contour of bare hull and base design bulbous we can see a higher water elevation for base design in comparison with bare hull in the bow of the ship that can be due the elevation of bulbous from base line and its height. In opposite to that there a decrease in the height of free surface behind the stern of the ship, mainly clear in the number of higher contour lines and the size of lower zones.

## Hydrodynamic optimisation of new hull bow shape by CFD code

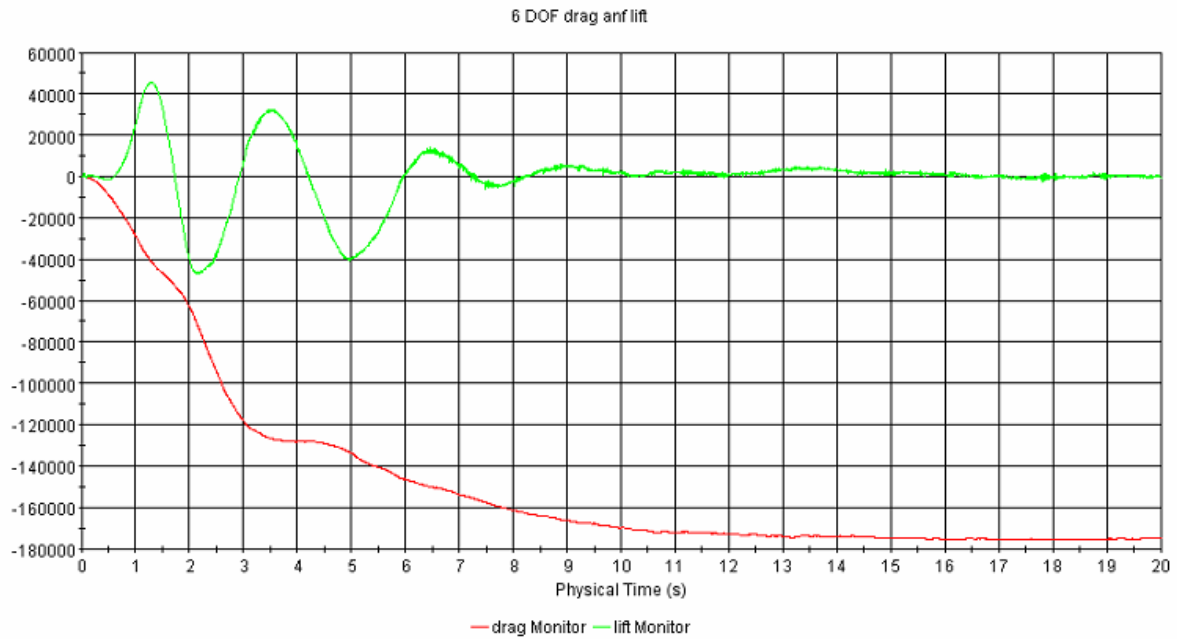


Figure 31: Drag and lift forces acting on base design for 25knts

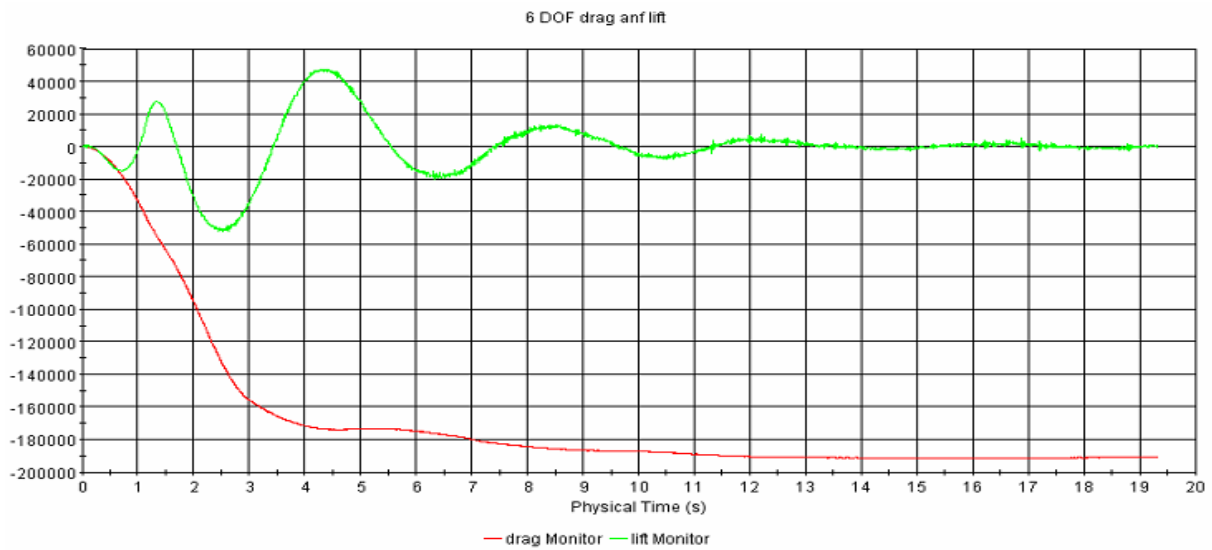


Figure 32: Drag and lift forces acting on Bare hull for 25knts

For the total drag forces, it is showing a reduction of 34 KN which is considered as an acceptable improvement of 8.75% with regards to bare hull resistance.

## 5.4 Generating designs for simulation test

### 5.4.1 Vehicle Sketch Pad (VSP)

Using VSP or vehicle sketch pad, this open source CAD software is used to build bulbous bow shape in order to integrate them in the bare hull form and then do the CFD simulation in STAR-CCM+.

Basically, it allows creating different geometries and also using profiles which can be used for symmetric cases.

For this project we needed to make a shape similar to the cut of bulbous bow in to make sections and give parameters or design variables to control the parametric generation of designs Based on the height, breadth and the length of sections by using functions controlling the parameters on different sections or by using a script instead of that .

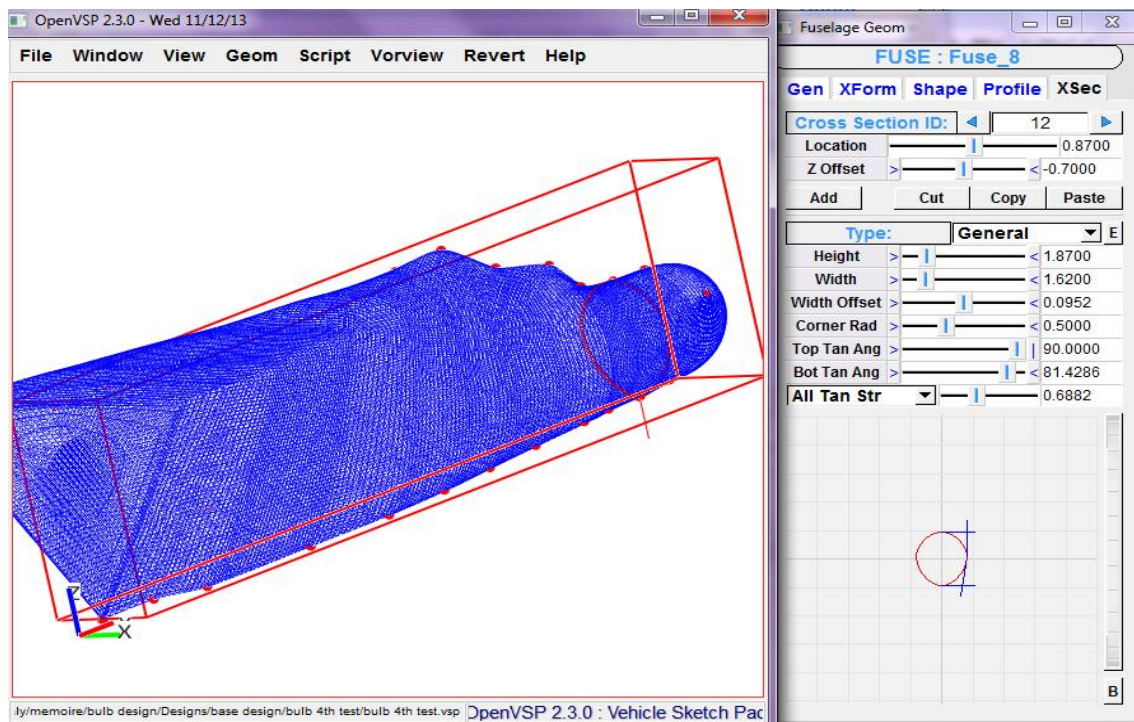


Figure 33: VSP overview task

First, we need to define the parameters to change according to our base design so for no complicated design is preferred to use simple parameters as it's shown in the blow figure:

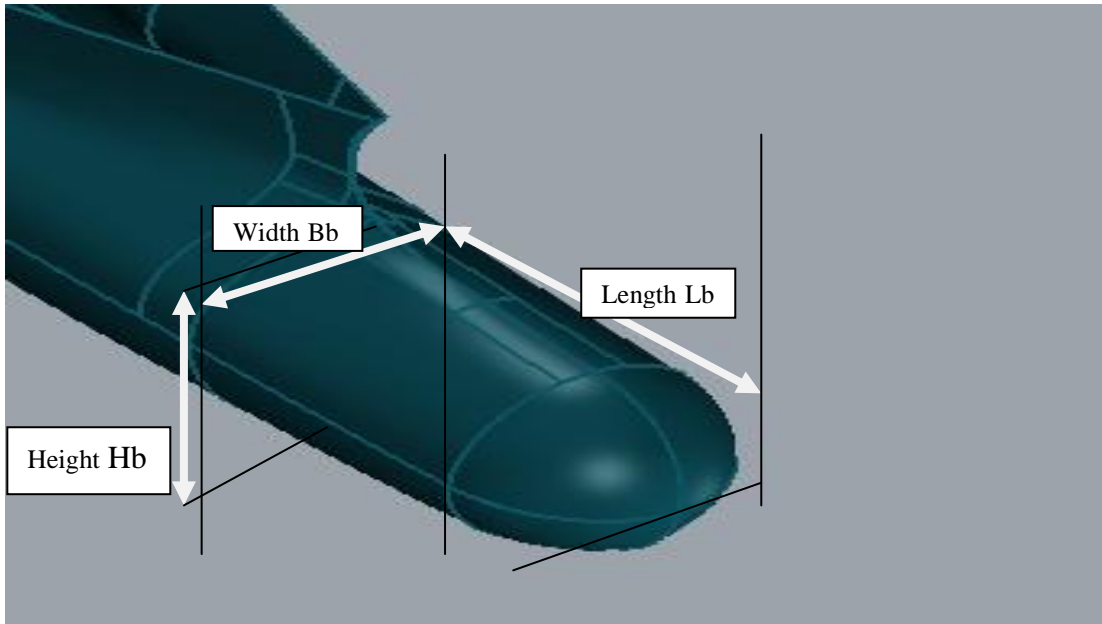


Figure 34: Parameters define generating design samples

### 5.5 Design of experiments

As explained above, the first phase of the design procedure consists in exploring the design space using a DOE approach. Therefore, a distribution of design points is generated. A first set of points, corresponding to moderate bow dimensions, the interval of parameters was not yet define till we get more information about the three different parameters and their influence on the objective.

Below table is showing the shapes and design parameters of 7 design samples, in addition to base design.


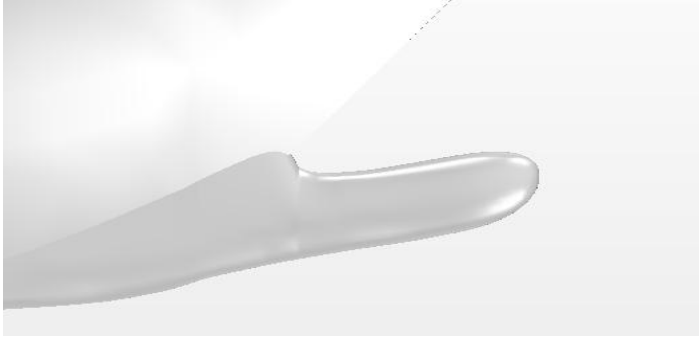
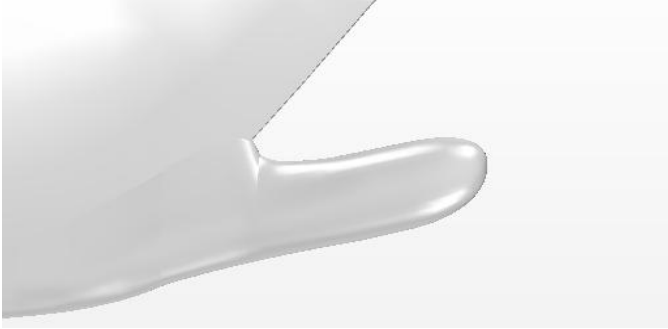
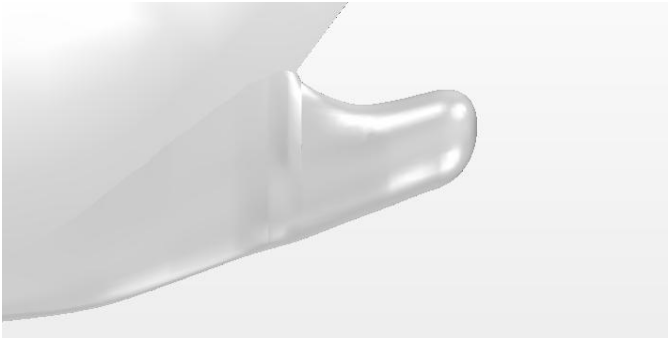
design	Dimensions parameters(m)	Design shape
Base Design	Lb=2.97 Hb=2.95 Bb=1.85	
Design_01	Lb=2.25 Hb=1.35 Bb=0.51	
Design_02	Lb=1.23 Hb=1.28 Bb=0.45	
Design_03	Lb=2 Hb=0.72 Bb=1.7	

Table 2: Design individuals' shapes and parameters

Hydrodynamic optimisation of new hull bow shape by CFD code

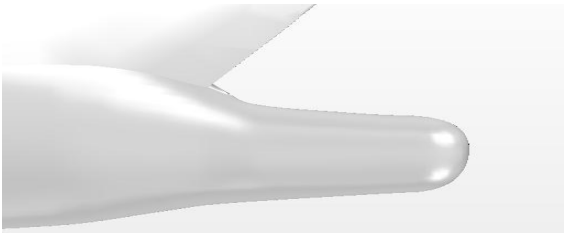
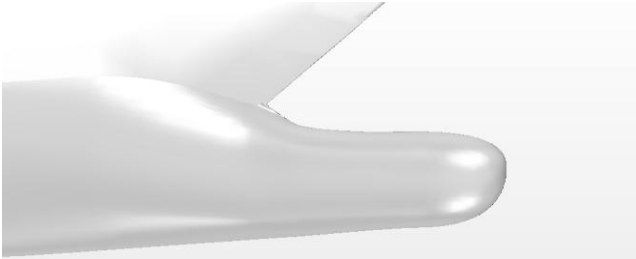
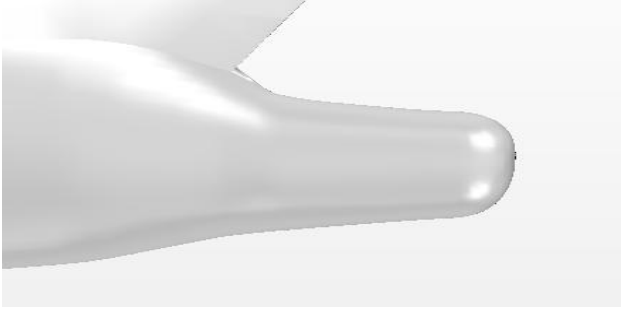
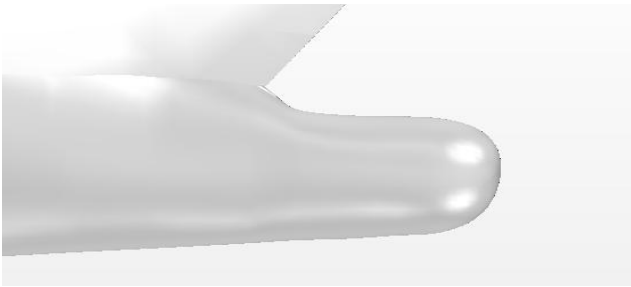
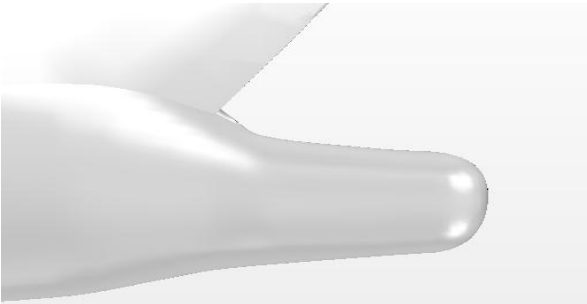
Design_04	<p>Lb=2.82</p> <p>Hb=2.2</p> <p>Bb=1.2</p>	
Design_05	<p>Lb=2.6</p> <p>Hb=2.25</p> <p>Bb=1.3</p>	
Design_06	<p>Lb=2.75</p> <p>Hb=2.15</p> <p>Bb=1.3</p>	
Design_07	<p>Lb=2.9</p> <p>Hb=2.4</p> <p>Bb=1.6</p>	
Design_08	<p>Lb=2.6</p> <p>Hb=2.5</p> <p>Bb=1.4</p>	

Table 3: Design individuals' shapes and parameters

### 5.6 Results of first design tests

After generating design samples on VSP, we can draw a DOE design of experiment for length Lb versus breadth, and Length Lb versus height Hb as shown in below figures.

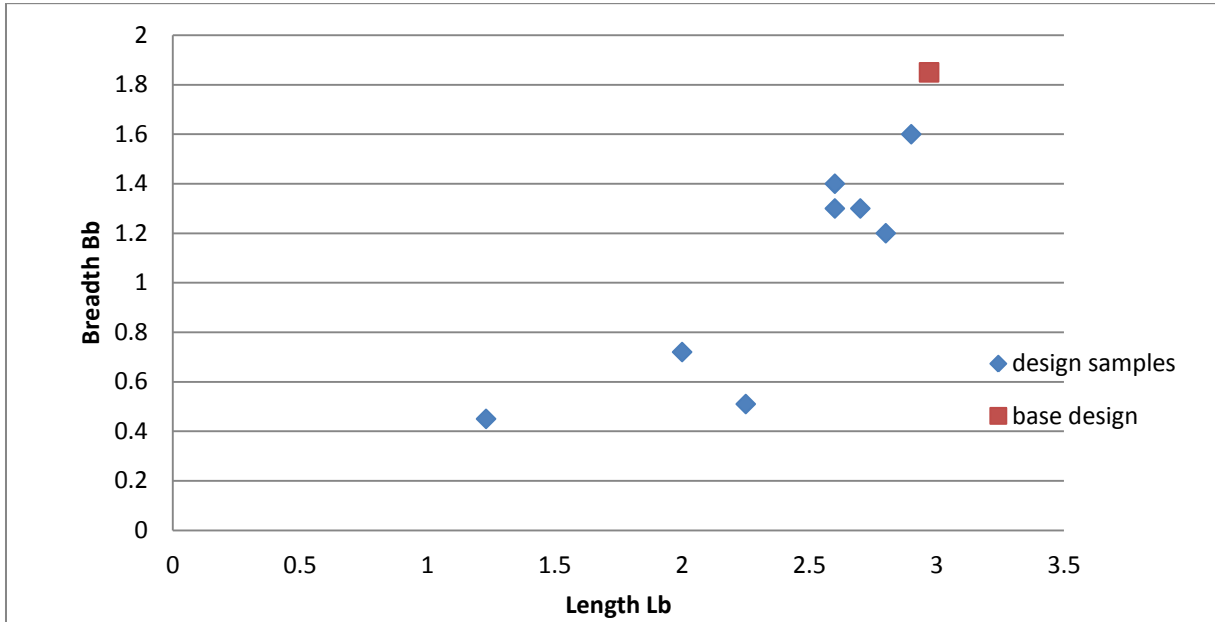


Figure 35 : DOE design of experiments represented by Lb versus Bb

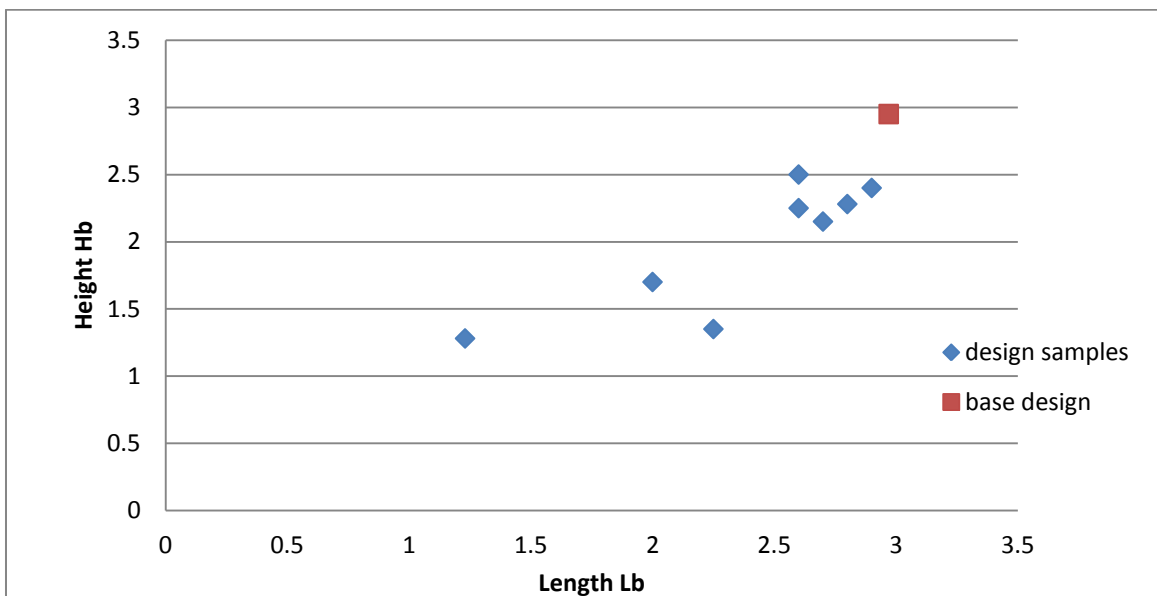


Figure 36 : DOE design of experiments represented by Lb versus Hb



## Hydrodynamic optimisation of new hull bow shape by CFD code

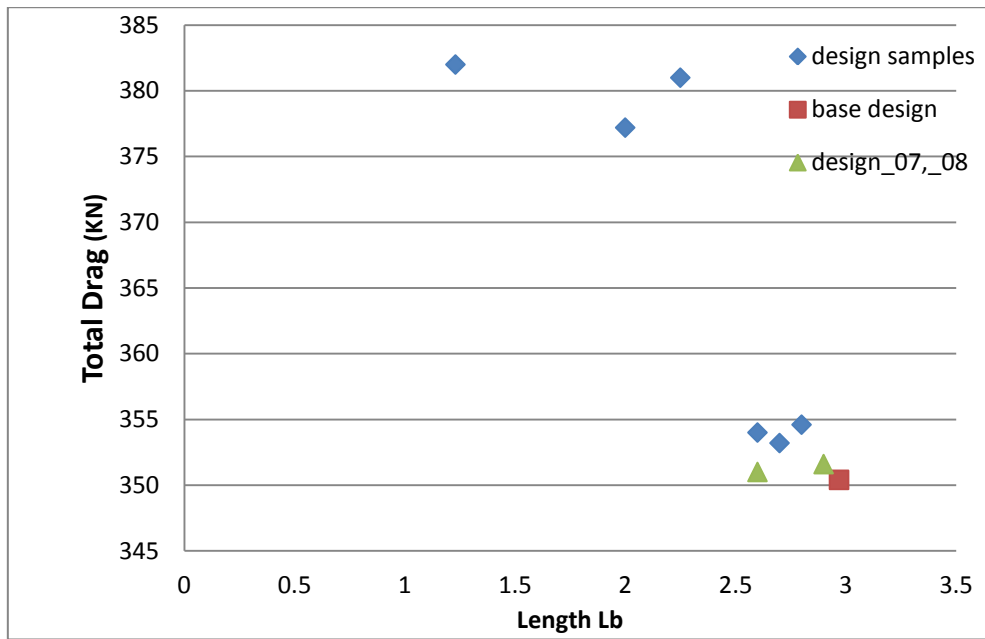


Figure 37 : Drag Resistance for different Lb of design individuals

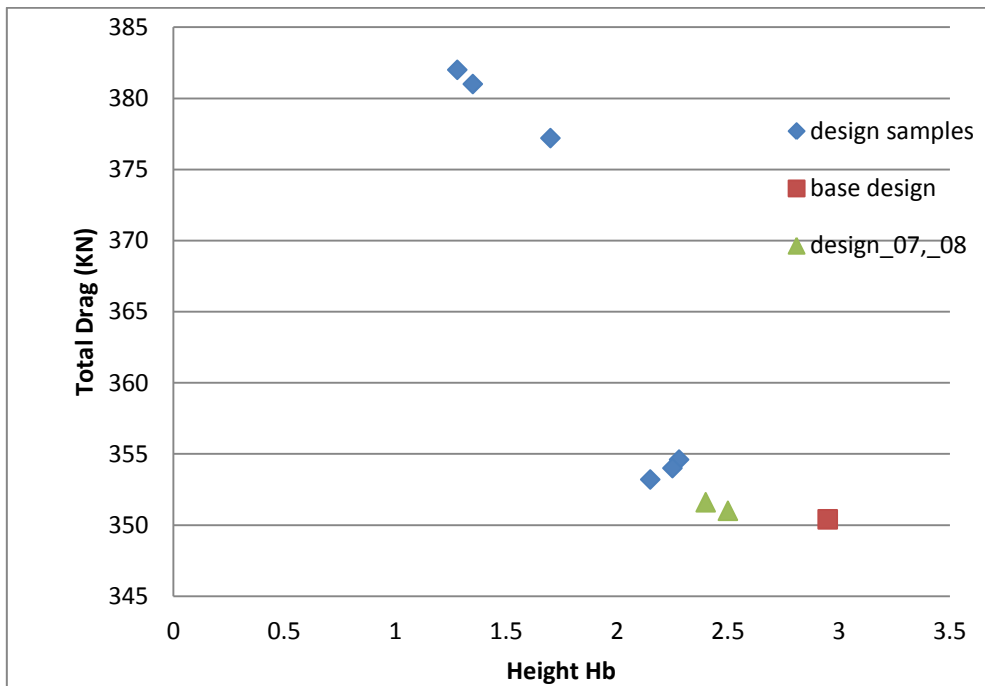


Figure 38: Drag Resistance for different Hb height of design individuals

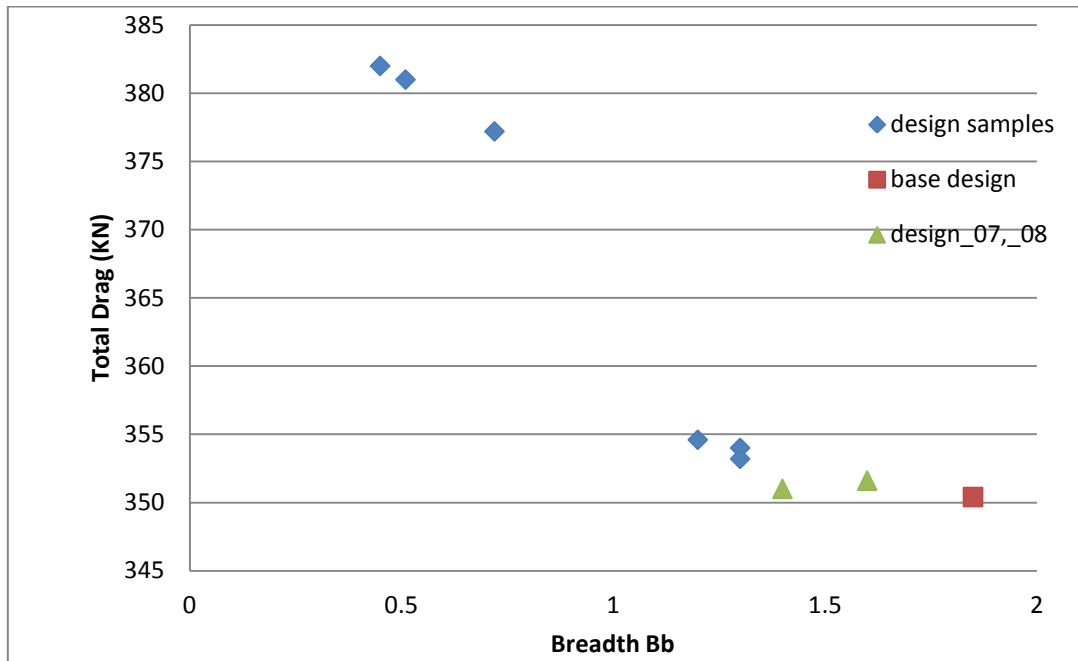


Figure 39: Drag Resistance for different Bb breadth of design individuals

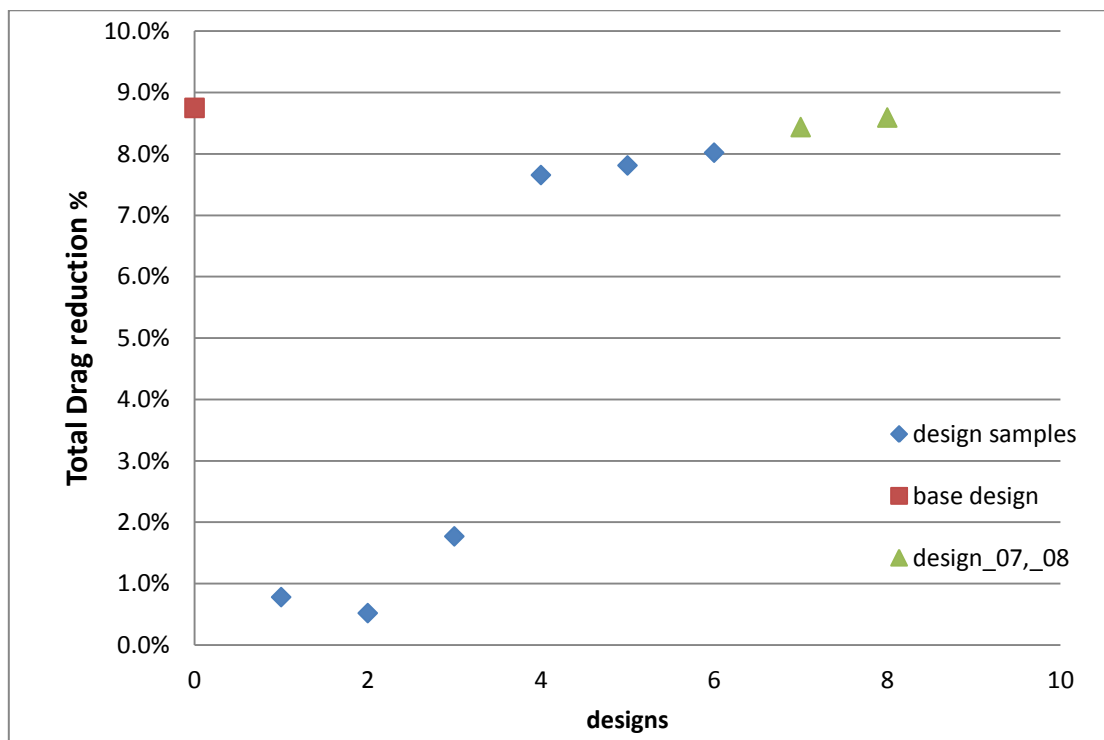


Figure 40 : Comparison of improvement in drag reduction with reference to bare hull

## Discussions and Conclusion

---

### 6.1 Discussion of results:

From the first design samples which have been taken for this optimisation study, we can say that:

- In variation of parameters of Lb, Hb and Bb of the individual designs from DOE figures (34 & 35), there is a clear approach to choose to take small values in comparison those of base design parameters, this is due to first assumption which may consider that base is somehow thick and wider enough as we can take its parameters as limit of range for parameters variation. But still we need to take more samples in the blank area shown from different DOE figures to get a full idea about the topology of the objective with regards to the three parameters.
- For the Drag resistance results, the first thing we can note is that base design still offering the best resistance for the ship with 8.75 %, also there are some useless design samples have been tested those with very small parameters values with very poor results (0.5% to 2%). In between we can find designs like design\_07 and design\_08 with close drag resistance results to base design but with different parameters mainly for the height Hb and the breadth Bb with. if we take as example design\_08 (Hb=2.5m, Bb=1.4 m and Lb= 2.6m) which has 8.6% of drag reduction, a small difference is missing to the best design so far.
- The difference between base and individual design tested also can be described by different bulb section profiles, considering base design has O shape profile and for the design samples were most of them of  $\nabla$  shape so by taking a new parameter range with the same shape will probably offer a better results.
- Another point should be considered is the jointment between bulb and hull which wasn't that perfect (not smooth enough, that can cause perturbations on the flow around the bulbous and physically adding resistance.

## 6.2 Conclusion:

A design optimisation procedure, based on a high fidelity CFD analysis tool of STAR-CCM+ has been used and applied to a realistic problem, dealing with the optimisation of the bow shape of a frigate vessel. The difficulty to automatically generate a bow shape from VSP CAD software was faced during this project but using a manual set of design parameters has been reported and has shown some admissible interval of design parameters.

A number of shape designs has been tested and compared with the base design to get the design of experiment DOE for the optimisation procedure which can be completed after this arriving to this point of project development, considered as preparation for the focused and the important step in this project

It seems from the first sample of DOE designs that, there is a change to decrease the volume of bulbous using another bulb section of nabla shape thinner than base section.

Nevertheless, this work demonstrates that for any optimisation study based on RANS code needs more time and more suitable CAD optimizer, in order to avoid lose time during design phase of the ship construction project.

## References:

- [1] C. Abt, S.D. Bade, L. Birk & S. Harries .September 2001 “Parametric hull form design –a step towards one week ship design” in 8th International Symposium on Practical Design of Ships and Other Floating Structures · PRADS 2001, Shanghai.
- [2] Francisco Pérez· José A. Suárez & Juan A. Clemente Antonio Souto in June 1, 2006 “Geometric modeling of bulbous bows with the use of non-uniform rational B-spline surfaces”, J Mar Sci Technol (2006).
- [3] Zhang Bao-Ji in July 23, 2008 “ the optimization of the hull form with the minimum wave making resistance based on rankine source method ”, science direct journal of hydrodynamics 2009,21(2):277-284 .
- [4] Shahid Mahmood & Debo Huang, in 2012 “Computational Fluid Dynamics Based Bulbous Bow Optimization Using a Genetic Algorithm”, Journal of Marine Science and Application (2012) 11: 286-294.
- [5] George Tzabiras & Konstantinos Kontogiannis in August 2009 “An integrated method for predicting the hydrodynamic resistance of low-Cb ships”, Computer-Aided Design Elsevier
- [6] Alfred M. Kracht, 1978 “Design of bulbous bows”, in 1978 Vol.86.
- [7] H.Schneekluth and V.Bertram in 1998 “Ship Design for Efficiency and Economy, Second edition”.
- [8] Mathieu Renaud & Luke Berry in 2013, “Ship design and optimisation with Computational Fluid Dynamics” Ship efficiency seminar - CMA CGM-HydrOcean1 (2013).